

**Utilizing SLAM and Innovative Adaptive Gripping Techniques as a Solution to
Material Handling Systems for Industries**

Thesis submitted to

Visvesvaraya National Institute of Technology, Nagpur

In partial fulfilment of requirement for the award of

degree of

Bachelor of Technology

(Mechanical Engineering)

by

Akshay Khatri BT11MEC012

Ashish Ghatge BT11MEC034

Anish Pimpley BT11MEC058

Kartikey Totewar BT11MEC080

Tushar Dhanwani BT11MEC083

Harshal Wankhede BT11MEC089

Guide

Dr. Shital Chiddarwar



Department of Mechanical Engineering

Visvesvaraya National Institute of Technology, Nagpur-440010(India) April 2015

Certificate

The thesis titled

**"Utilizing SLAM and Innovative Adaptive Gripping Techniques as a Solution to
Material Handling Systems for Industries"**

Submitted by

Akshay Khatri	BT11MEC012	Ashish Ghatge	BT11MEC034
Anish Pimpley	BT11MEC058	Kartikey Totewar	BT11MEC080
Tushar Dhanwani	BT11MEC083	Harshal Wankhede	BT11MEC089

For the award of degree of Bachelor of Technology has been carried out under my supervision at the Department of Mechanical Engineering of Visvesvaraya National Institute of Technology, Nagpur. The work is comprehensive, complete and fit for evaluation.

Dr. Shital Chiddarwar,

Asst. Professor

Department of Mechanical
Engineering, VNIT, Nagpur.

Head,

Department of Mechanical Engineering,
VNIT, Nagpur.

Date:

Declaration

We, hereby declare that the thesis titled “Utilizing SLAM and Innovative Adaptive Gripping Techniques as a Solution to Material Handling Systems for Industries” submitted herein has been carried out by us in the Department of Mechanical Engineering of Visvesvaraya National Institute of Technology, Nagpur. The work is original and has not been submitted earlier as a whole in part for the award of any degree/diploma at this or any other Institute/University.

Akshay Khatri

Ashish Ghatge

Anish Pimpley

Kartikey Totewar

Tushar Dhanwani

Harshal Wankhede

Date:

Acknowledgements

With immense pleasure and great respect, we express our gratitude to Dr. Shital Chididarwar of Department of Mechanical Engineering VNIT, Nagpur for her invaluable guidance, inspiration and constant encouragement throughout the project work.

We also express our sincere gratitude towards Dr. K. M. Bhurchandi, of Electronics Engineering Department VNIT, for generous guidance and motivation from the beginning to the completion of the project.

ABSTRACT

Most existing material handling robot designs occupy the ends of the spectrum, by being either affordable & rigid or flexible & expensive. The research intends to find a solution to the duality, as a material handling robot that achieves maximum versatility and reliability at minimum monetary expense has been designed. Kinect input is autonomously utilized from SLAM render generation, identification of object position and corresponding arm orientation for approach. The robot is mounted on a movable platform for navigation. The robotic end effector innovates on 2 distinct fronts, finger alignment and adaptive contact surfaces. The proposed gripper finger alignment offers solutions to shortcomings of popular standard designs and the adaptive contact surfaces ensure robust and reliable gripping, all while remaining affordable and feasible for manufacturing.

TABLE OF FIGURES

- Figure 1.1: A forklift Involved in Material Handling
- Figure 1.2: On Rail Transfer Carts used to move heavy materials
- Figure 1.3: Conveyor Belts
- Figure 1.4: Automated Storage and Retrieval System
- Figure 1.5: Automated Guided Vehicle
- Figure 3.1: Parts of a Robotic Manipulator
- Figure 3.2: Structure of a Robotic Manipulator
- Figure 3.3: Developing Kinematic models for Forward and Inverse Kinematics
- Figure 3.4: Shows the Link Parameters
- Figure 3.5: The four parameters of DH convention are as shown in the figure
- Figure 3.6: Initial CAD Model showing the basic design of the arm
- Figure 3.7: Position of Kinect on the platform
- Figure 3.8: Block Diagram of the System
- Figure 3.9: Link1 – Base link with the movable platform
- Figure 3.10: Link2 – The link with the pulley assembly
- Figure 3.11: Link 3
- Figure 3.12: Bearing – press fitted on the moving platform
- Figure 3.13: Big Pulley
- Figure 3.14: Small Pulley
- Figure 3.15: Servomotor HS-805MG
- Figure 3.16: Platform – Bottom Half
- Figure 3.17: Robot Wheels
- Figure 3.18: Timing Pulley Slice

Figure 3.19: Joining Plate (Acrylic) – Specifically made for the proper mounting of the pulley and motor

Figure 3.20: Frame Allocation on the joints

Figure 3.21: Different singularity conditions observed by the arm

Figure 3.22: Final CAD Model

Figure 4.1: Index for gripper

Figure 4.2: Gripper (Earlier Design) – Basic Diagram with gears

Figure 4.3: Gripper (Final Design) – With parallel link mechanism

Figure 4.4: Mathematical Diagram of gripper

Figure 4.5: Working diagram of the finger in different positions

Figure 4.6: Schematic diagram showing gripper grabbing a spherical object

Figure 5.1: Depicts arrangement of wheel and encoder motors at the bottom of the moving platform

Figure 5.2: Shows motor to be placed on the platform with movable platform arrangement

Figure 5.3: Arm assembly (without platform and gripper)

Figure 5.4: Placement of 2nd and 3rd motor with aluminium angles

Figure 5.5: Arrangement of timing pulleys and belts to drive the 3rd joint by 3rd motor placed at the 2nd Joint

Figure 5.6: Power transmission from 1st belt to the 2nd

Figure 5.7: A gear being made by the 3D printer – PLA plastic

Figure 5.8: 3D printer

Figure 5.8: 3D printed parts of the Palm

Figure 5.8: Parallel gripping palm (Without motor)

Figure 5.8: The picture shows adaptive finger assembly and the 3rd finger at the bottom

Figure 6.1: Overview of two different RGB-D SLAM approaches

Figure 6.2: The Kinect and its main components

Figure 6.3: Emitted pattern of speckles by the Kinect

Figure 6.4: Schematic representation of depth-disparity relation

Figure 6.5: Basic concept of vSLAM

Figure 6.6: Odometry system

Figure 6.7: Photo of the hardware and the output in rviz of the mapping module

Figure 6.8: RGB image on the left and depth image on the right

LIST OF TABLES

Table 3.1: Joint Angle Range

Table 3.2: Values of d-h parameters for the arm

Table 4.1: Comparison between grippers based on type of input energy for gripping

Table 4.2: Comparison between grippers based on no. of fingers or their placements

Table 4.3: Coefficient of friction between different materials

Table 6.1: Kinect specifications

Table 6.2: Approximate values of the Kinect Field of View (FoV) in degrees

CONTENTS

Abstract

Table of figures

List of tables

Contents

1 INTRODUCTION	1
1.1 Existing technologies	2
1.2 Problems with the existing technologies	5
1.3 Objectives of material handling systems	6
2 DESIGN STATEMENT	7
3 ROBOTIC ARM	8
3.1 What are robotic manipulators?	8
3.2 Classification	9
3.3 Manipulator structure	10
3.4 Kinematic Modeling of the Manipulator	11
3.5 Direct Kinematics	12
3.6 Inverse Kinematics	16
3.7 The design	16
4 ROBOTIC GRIPPER	33
4.1 Index	33
4.2 Introduction	33
4.2.1 What is a Gripper or End effector?	33
4.2.2 Existing technology	34
4.3 The gripper	34
4.3.1 The arrangement	34

4.3.2 Comparison gripper base model's parameters	35
4.3.3 Summary and conclusion	36
4.3.4 Design considerations	37
4.3.5 Base Schematic	37
4.3.6 Advantages over standard designs	38
4.3.7 Final render	38
4.4 The palm	39
4.4.1 Concept	39
4.4.2 Mathematical modelling	39
4.5 The Fingers	42
4.5.1 Concept	42
4.5.2 Mathematical modelling	44
5 FABRICATION	46
5.1 Mobile Platform	46
5.2 Robotic arm	47
5.3 The Gripper	51
6 SLAM BASED NAVIGATION	56
6.1 Introduction	56
6.1.1 Related Work	56
6.2 The Microsoft Kinect	59
6.2.1 Depth Measurement	60
6.2.2 Triangulation model	61
6.2.3 Kinect Data Accuracy	62
6.2.4 Precision and Resolution	62
6.3 Applications in Mobile Robotics	63
6.3.1 Obstacle Avoidance and Collision Detection	63

6.3.2	Localization and Navigation	64
6.4	Kinect on ROS	64
6.4.1	Robot Operating System (ROS)	64
6.4.2	ROS and the Kinect	65
6.5	Proposed System	65
6.5.1	Vision based SLAM	65
6.5.2	Odometry System	66
6.5.3	Mapping	66
7	RESULT	69
8	FUTURE SCOPE	70
9	BIBLIOGRAPHY	71

1 INTRODUCTION

Material handling is a necessary and significant component of any productive activity. Material handling means providing the right amount of the right material, in the right condition, at the right place, at the right time, in the right position and for the right cost, by using the right method. It is simply picking up, moving, and laying down of materials through manufacture. It applies to the movement of raw materials, parts in process, finished goods, packing materials, and disposal of scraps. In general, hundreds and thousands tons of materials are handled daily requiring the use of large amount of manpower while the movement of materials takes place from one processing area to another or from one department to another department of the plant. The cost of material handling contributes significantly to the total cost of manufacturing.

In the modern era of competition, this has acquired greater importance due to growing need for reducing the manufacturing cost. The importance of material handling function is greater in those industries where the ratio of handling cost to the processing cost is large. Today material handling is rightly considered as one of the most potentially lucrative areas for reduction of costs. A properly designed and integrated material handling system provides tremendous cost saving opportunities and customer services improvement potential.

Industries often involve handling of multiple parallel projects and working on each of which requires a new set of training skilled labour in object identification, segregation and sorting. Industries with large shop floors, due to the restriction of how much a single person can remember or grasp, have to compulsively bifurcate cohesive environments into multiple subsections. A well known postulate, "Higher the number of parts, lower the efficiency", comes into play here as hand off between section can often be slow due a massive number of managerial hoops to jump through. As compared to humans, functioning of an automated machine is absolute. It is never late, and works with near perfect efficiency, as long as proper design and programming is in order.

Thus, we aim to design a material handling robot that shall suit the needs of the industry.

1.1 EXISTING TECHNOLOGIES

Existing material handling technologies include:

Forklift – Industrial trucks often involved in material handling. They require manual handling and human intervention throughout the material handling process.



Figure 1.1: A forklift Involved in Material Handling

On-rails transfer cart - It moves on the rails and can transfer heavy cargoes or equipment with the weight 1-300tonnes between the workshops or warehouses in the factory.



Figure 1.2: On Rail Transfer Carts used to move heavy materials

Conveyors - Conveyors can be used in a multitude of ways from warehouses to airport baggage handling systems. Some types of conveyors are power and free, chain, towline and roller conveyor.



Figure 1.3: Conveyor Belts

Cantilevered crane loading platforms – They are temporary platforms attached to the face of multi-storey buildings or structures to allow materials and equipment to be directly loaded on or shifted off floor levels by cranes during construction or demolition.

Automated Storage and Retrieval Systems – AS/RS are used for automatically loading and retrieving objects/loads from different storage locations. They involve variety of computer controlled systems used for handling massive amount of loads being moved into and out of storage.



Figure 1.4: Automated Storage and Retrieval System

Automated Guided Vehicle - It is a mobile robot that follows markers or wires in the floor, or uses vision, magnets, or lasers for navigation. It often involves laying an entire series of markings in order to guide its path around the shop floor from the storage unit to the area of work and vice versa.



Figure 1.5: Automated Guided Vehicle

1.2 PROBLEMS WITH THE EXISTING TECHNOLOGIES

A good management practice is to weigh benefits against the limitations or disadvantages before contemplating any change. Existing Material handling systems also have consequences that may be distinctly negative. These are

- Huge additional/initial investment required.
Eg. Use of Conveyor belts involve construction of the guide ways or rails leading to increase in the overall cost of the material handling system
- Lack of flexibility
Eg. Automated Guided Vehicles often involve following a particular path/line already constructed during the establishment of the factory. Thus the path of AGV is pre-defined and inflexible to change which is often needed in the industries.
- Additional maintenance staff and cost
Additional staff and trained workers are required in order to drive/ supervise/maintain the systems as often they involve manual interference in order to operate properly.
- Cost of auxiliary equipment.
The additional equipments required often lead to higher costs.
- Space and other requirements
AS/RS (Automated storage and retrieval system), conveyor belts, overhead automated line hangers, etc often utilize a huge amount of space leading to, either the need for a large area for shop floor or cramping up of the existing area which may lead to inadequate work environment adversely affecting productivity or leading to industrial accidents.

These are only some of the problems associated with the existing material handling systems which inspired us to think about better and more effective ways for handling materials supplementing better productivity.

1.3 OBJECTIVES OF MATERIAL HANDLING SYSTEMS

- To reduce manufacturing cycle time
- To provide better control for the flow of materials
- To be flexible in order to efficiently adapt to the changing work environment or shop floor design.
- To reduce delays and damage to properties or human resources to avoid accidents
- Promote productivity – finding the shortest path possible every time from the storage space to work space and modify and alter path adapting to new and changing work environment.
- Avoiding generation of bottleneck so as to maintain smooth flow of the line
- Automation of material handling as much as possible in order to avoid using excess/redundant workers and also avoid lethargy in performing work often created by using human workers.

So the above objectives that are needed to be achieved for material handling and the problems associated with the existing material handling equipments motivated us to pursue an innovative project in this field comprising of all the solutions required for a material handling system in the industry, thus creating a complete solution and most efficient solution for handling the materials.

2 DESIGN STATEMENT

The objective of the project is to design an automated robot for object sorting and transportation in industries. The parts of the robot can be categorized based on function as follows, Chassis as the base, Vehicle for transportation, SLAM for 3D mapping and path generation, Kinect for object location, arm for approaching the object and the gripper for grabbing the object. The functioning of the robot begins with an input to SLAM, which refers to a render to map the ideal path to the object. The Kinect mounted on the vehicle then provides the co-ordinates of the object with respect to the vehicle. These co-ordinates are used to find the angles for rotation of the robotic arm links. Once, the arm has approached the object, the gripper grabs the object and the vehicle return to the user along with the object to be retrieved.

3 ROBOTIC ARM

3.1 WHAT ARE ROBOTIC MANIPULATORS?

Manipulator: In robotics a manipulator is a device used to manipulate materials without direct contact.



Figure 3.1: Parts of a Robotic Manipulator

A robotic arm is a type of mechanical arm, usually programmable, with similar functions to a human arm. It is nothing but an open or closed kinematic chain of rigid links interconnected by movable joints. In some configurations, links can be considered to correspond to human anatomy as waist, upper arm and forearm with joints at shoulder and elbow. At the end of the arm, a wrist joint connects the end effector to the forearm. An end-effector maybe a gripper or a tool depending on the function that is required to be performed by the arm.

3.2 CLASSIFICATION

The robotic arm can be classified based on

- The degree of freedom (No. of independent motions possible i.e. no. of joints) Based on the requirements, the arm maybe 3/4/5/ 6 degree of freedom or a redundant arm.
 - Constrained Manipulators: Manipulators having less than 6 DOF. The industrial robots are generally 4 or 5 DOF manipulators.
 - Spatial Manipulator- 6 DOF
 - Redundant Manipulator- greater than 6 DOF. In order to create redundancy i.e. to avoid obstacles coming inside the workspace, the DOF of the arm maybe more than 6.
- by arm configuration
 - Rectangular Co-ordinates – The robot can move along X, Y, Z axis on a straight line.
 - Cylindrical Co-ordinates - The robot manipulator can rotate about its base and move along straight line in the other axes.
 - Polar Co-ordinates – The manipulator can rotate about its base as well as its head. It can also move in and out.
 - Articulated Configuration
- Type of controller
- Type and number of joints.
- Motion of the joints
 - Planar Manipulator- Considers movement of 1 joint at a time.
 - Spatial Manipulator- Considers simultaneous movement of the required number of joints

3.3 MANIPULATOR STRUCTURE:

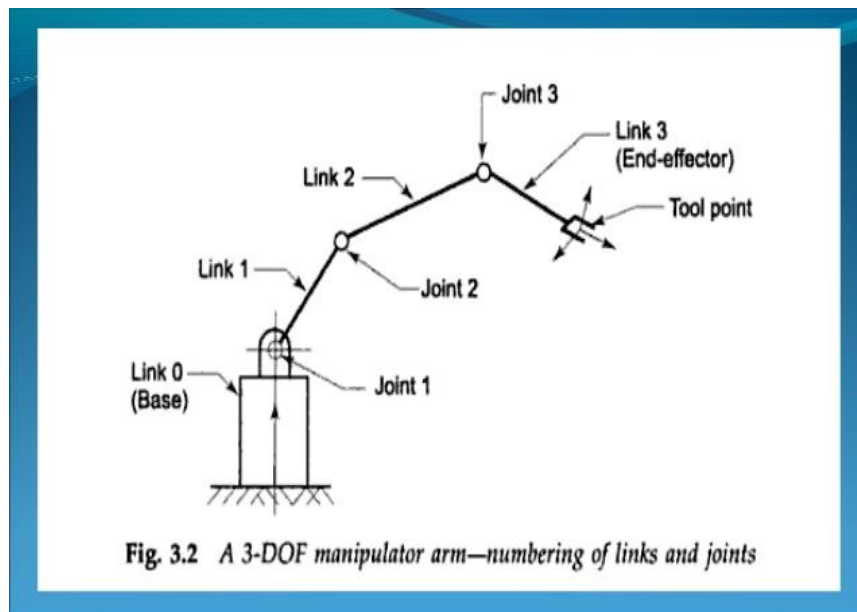


Figure 3.2: Structure of a Robotic Manipulator

The robot anatomy may differ for open chain and closed chain serial kinematic manipulators and also for parallel manipulators.

Our project takes into consideration an open chain serial kinematic manipulator.

It consists of rigid links joined together by revolute joints (rotary motion) or prismatic joints (linear motion). The number of DOFs a manipulator possesses is the number of independent parameters required to completely specify its position and orientation in space. Because each joint has only one DOF, the degrees of freedom of a manipulator are equal to the number of joints.

As seen in the diagram above, the links are numbered as mentioned with the base link numbered '0'. The joints are numbered starting from '1' till 'n' where 'n+1' are the number of links.

3.4 KINEMATIC MODELING OF THE MANIPULATOR

Kinematical modelling is the analytical description of the geometry of motion of the manipulator with respect to a fixed frame/reference frame as a function of time. It creates a relation between the joint variables and position and orientation of the end-effector so as to control the trajectory of the end-effector and manipulate objects in the workspace.

This can be further subdivided in two categories

Forward kinematics: It is the problem of finding the position and orientation of the end effector with respect to the reference frame (generally at the immobile base link) given the set of joint link parameters. Here we generate equations in order to find out the position and orientation of the end effector. It gives us the position and orientation of the end effector as a function of joint variables and other joint link parameters.

Inverse Kinematics: Given the position and orientation of the end-effector (with respect to the immobile base) we can find the set of joint variables responsible to bring the end effector there in the first place. Inverse kinematics techniques can be used in order to form solution to these problems.

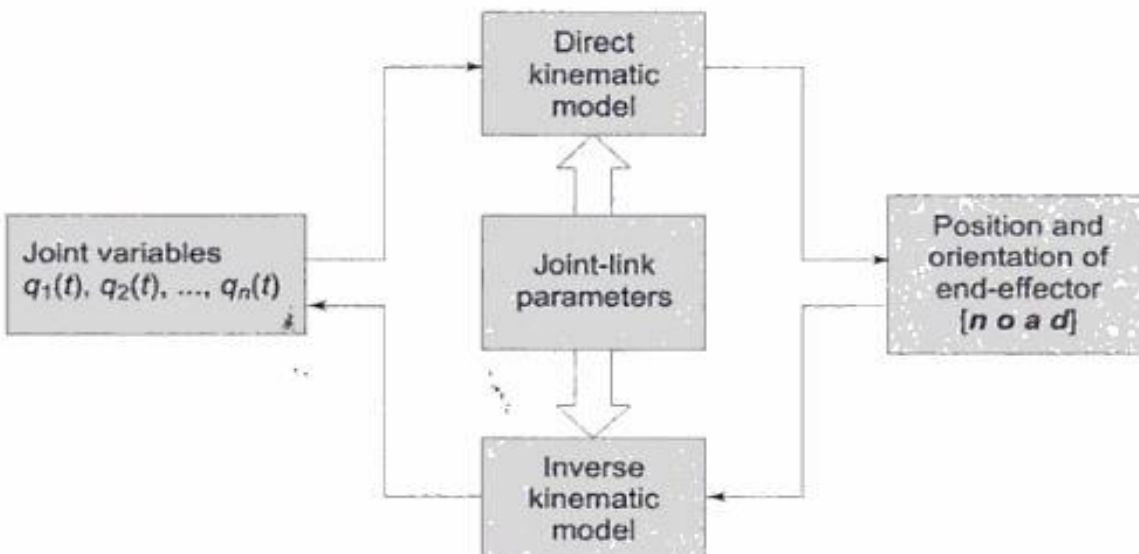


Figure 3.3: Developing Kinematic models for Forward and Inverse Kinematics

Finding the position and orientation of individual links (joint angles) having known the position and orientation of the end-effector is the ultimate aim of the mathematical modelling of the arm. However in order to perform inverse kinematics, one needs to create a direct kinematic model in order to generate a set of equations in a homogeneous matrix so as to compare with the actual known position and thus proceed. So in the beginning we will see how to perform Direct Kinematics.

3.5 DIRECT KINEMATICS:

A co-ordinate frame is attached to each link, like frame $\{i\}$ to link i in order to describe the position and orientation of the link. The diagram shows link i associated with joint axes $(i-1)$ and i .

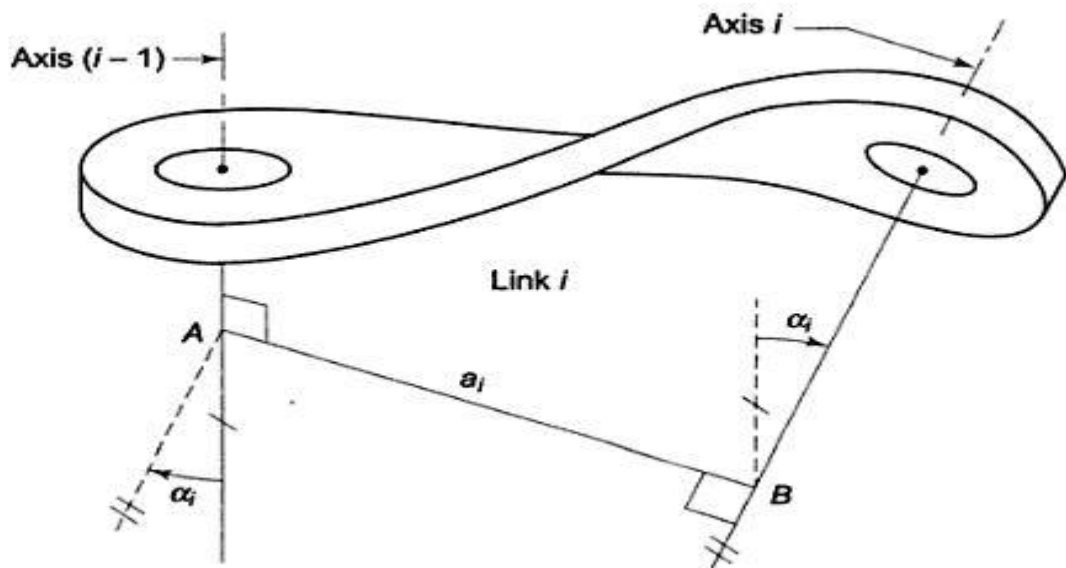


Figure 3.4: Shows the Link Parameters

Firstly, we will understand what are Link and Joint Parameters.

Link Parameters:

a_i - link length.

It is the mutual perpendicular which gives the shortest distance between the two joint axes.

α_i - link twist angle.

The angle between projection of axis (i-1) and axis(i), on a plane perpendicular to common normal AB is known as the link twist angle.

These link parameters are constant for a given link.

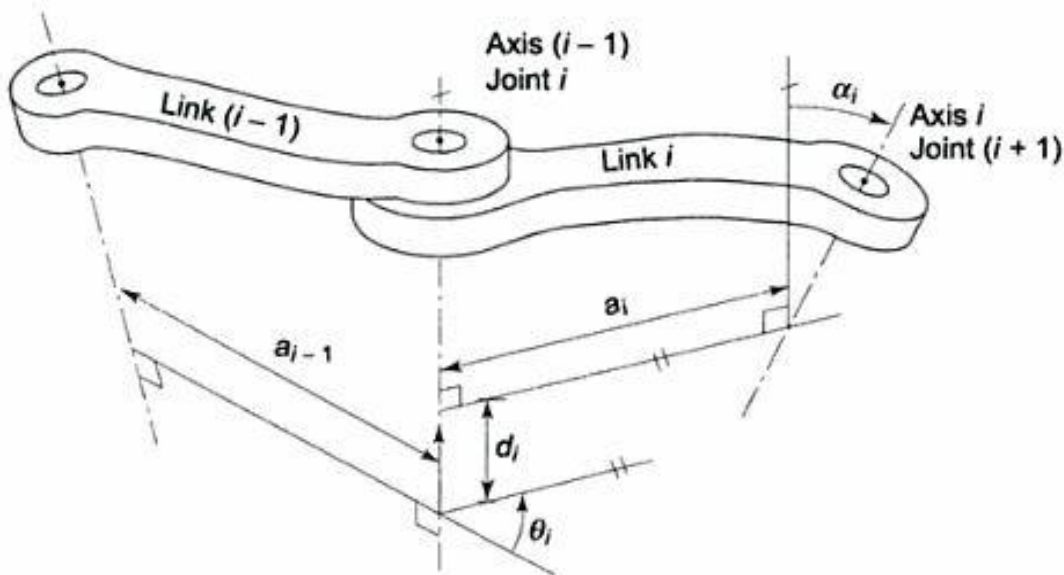


Figure 3.5: The four parameters of DH convention are as shown in the figure.

Joint Parameters:

d_i - Joint Distance

It is the perpendicular distance between the two adjacent common normals a_{i-1} and a_i measured along axis a_{i-1} .

Θ_i - Joint Angle

It is the angle between the two adjacent common normals a_{i-1} and a_i measured along right hand sense about axis a_{i-1} .

Denavit – Hartenberg Notations

The dh parameters method is used in order to allocate frames at every joint of the arm and create an overall transformation matrix.

Figure shows a pair of adjacent link (i-1) and link i, their associated joints, joints (i-1), i, (i+1), and axes (i-2), (i-1) and i, respectively. Line AB in the figure, is common normal to (i-2) and (i-1) axes and line CD is the common normal to (i-1) and i-axes. A frame {i} is assigned to link I as follows:

- (i) The z_i -axis is aligned with axis i, its direction being arbitrary. The choice of direction defines the positive sense of joint variable Θ_i .
- (ii) The x_i -axis is perpendicular to z_{i-1} -axis and z_i and points away from axis z_{i-1} -axis, that is, x_i -axis is directed along the common normal CD.
- (iii) The origin of the ith coordinate frame, frame {i}, is located at the intersection of axis of joint (i+1), that is, axis I, and the common normal between axis (i-1) and I (common normal is CD), as shown in the figure.
- (iv) Finally y_i -axis completes the origin the right-hand orthonormal coordinate frame {i}.

Note that the frame {i} for link i is at the distal end link i and moves with the link.

With respect to frame { i-1} and frame {i}, the four DH-parameters- two link parameters (a_i , α_i) and two joint parameters (d_i , Θ_i)-are defined as:

- (a) Link Length (a_i)-distance measured along x_i -axis from the point of intersection of x_i -axis with z_{i-1} -axis (point C) to the origin of frame {i}, that is, distance CD.
- (b) Link twist (α_i)-angle between z_{i-1} -axis and z_i -axis measured about x_i -axis in the right-hand sense.
- (c) Joint distance(d_i)-distance measured along z_{i-1} -axis from the origin of frame {i-1} (point B) to the intersection of x_i -axis with z_{i-1} -axis (point C), that is, distance BC.
- (d) Joint angle (Θ_i)-angle between x_{i-1} -and z_i -axes in the right-hand sense.

These outlined attachments of frame are in general and do not lead to a precise frame allocation. Thus using the D-H parameter rules for frame assignment, we can avoid this ambiguity to a greater extent. These frame allocation rules and allotment of D-H parameters are used in order to perform the kinematics of our manipulator.

Manipulator transformation matrix

A transformation matrix is a matrix relating the two frames attached to the links.

A transformation matrix of frame (i-1) and frame (i) consist of 4 basic transformations

- A rotation about z_{i-1} axis by an angle Θ_i .
- Translation along z_{i-1} by distance d_i .
- Translation by distance a_i along x_i axis.
- Rotation by an angle α_i about x_i axis.

So we get a generalised form of the transformation matrix as

$${}^{i-1}\mathbf{T}_i = \begin{bmatrix} C\theta_i & -S\theta_i C\alpha_i & S\theta_i S\alpha_i & a_i C\theta_i \\ S\theta_i & C\theta_i C\alpha_i & -C\theta_i S\alpha_i & a_i S\theta_i \\ 0 & S\alpha_i & C\alpha_i & d_i \\ 0 & 0 & 0 & 1 \end{bmatrix}$$

Thus the position and orientation of the tool frame relative to the base frame can be found by considering the n consecutive link transformation matrices relating frames fixed to adjacent links. Thus we get

$${}^0\mathbf{T}_n = {}^0\mathbf{T}_1 * {}^1\mathbf{T}_2 * \dots * {}^{n-1}\mathbf{T}_n.$$

3.6 INVERSE KINEMATICS:

There are various techniques that can be used to solve the problem of inverse kinematics. But one of the most appropriate and trusted method avoiding multiple solutions as much as possible as is ‘Closed Form Solution technique’. For our manipulator, we use ‘closed form solution technique’ so as to find out the joint angles when position and orientation of gripper is known.

3.7 THE DESIGN

The arm designed and developed is a 3 Degree of Freedom serial kinematic chain with RRR (R-Revolute) configuration. The system doesn’t need larger degrees of freedom for creating redundancy as it is capable of attaining the same with the help of the mobility of the platform.

Advantage of the arm over traditional manipulators:

- The lower DOF, reduces the computational efforts as well as the complexity of inverse kinematics.
- All the motors of the arm are fitted at the base thus bringing the center of gravity at the lowest possible position and thus maintaining stability throughout the operating conditions.

- Also, it increases the weight bearing capacity of the arm as the weight of the motors do not induce torque, thus decreasing the torque requirement of the motors & bringing down the overall cost.

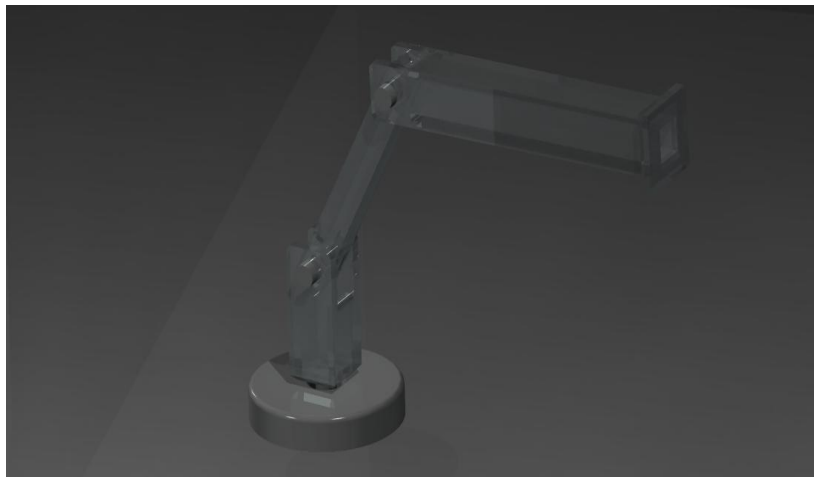


Figure 3.6: Initial CAD Model showing the basic design of the arm

Belt and Pulley Assembly

Along with the Joint 1, the Joint 2 too is driven by servo motor placed at Joint 1 with the help of timing belts. The timing belt and pulley mechanism is used to transmit power from Joint1 to Joint2 without the need of placing the 2nd servo motor at Joint2. The timing belts are incorporated in our design as they offer no relative motion between the two meshing entities i.e. avoid slippage which gives precise motion to the arm with least amount of errors.

In order to accommodate the required length of Link2 in our design, we used two belts instead of one due to lack of availability of the required dimensions of the belt. The arrangement can be seen in the assembly photos in the later part of this thesis.

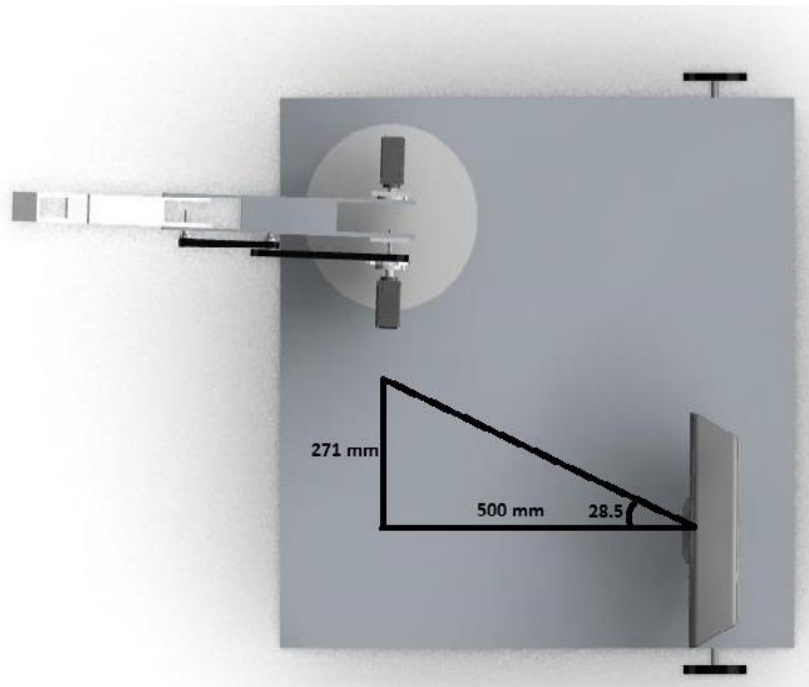


Figure 3.7: Position of Kinect on the platform

Kinect can detect objects at a minimum distance of 500 mm. Thus the Kinect is placed on the platform, 500 mm behind Joint 1 axis. Also considering the horizontal field of vision of Kinect (57 degrees) it is to be placed at an appropriate distance so that the arm doesn't obstruct its field of vision. The position of Kinect can be seen in the figure.

To ensure the coincidence of the center of gravity of the robot with the longitudinal central axis of the vehicle, the circuit is positioned to offset the CG shift introduced by the off center locations of the arm and Kinect.

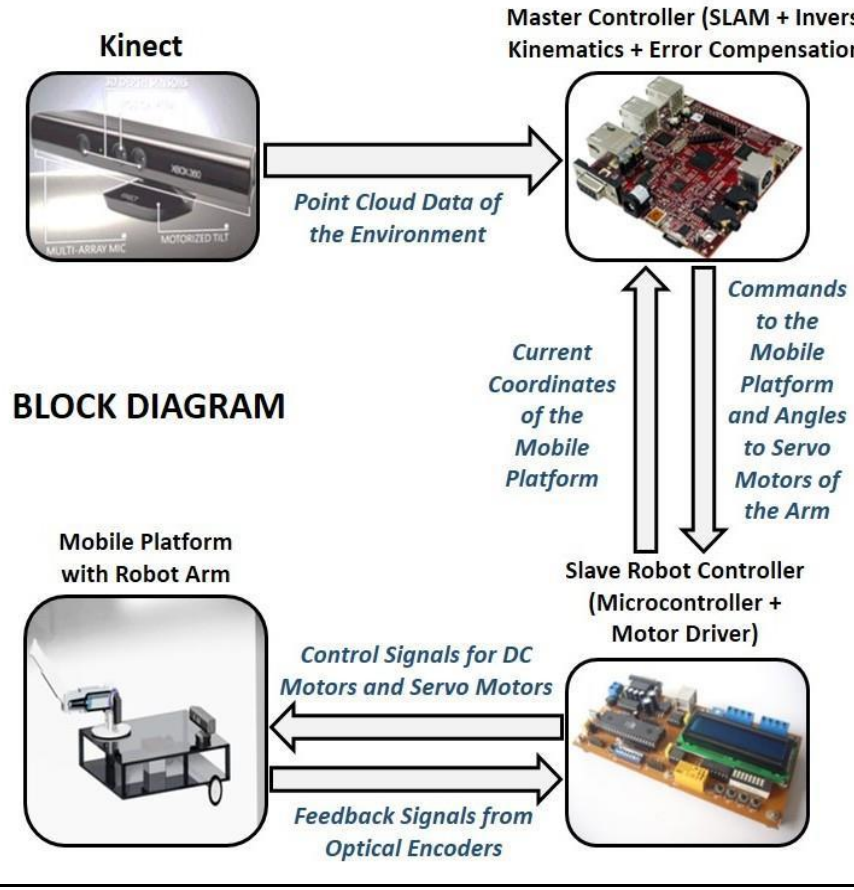
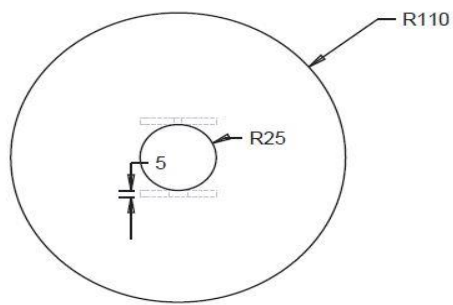
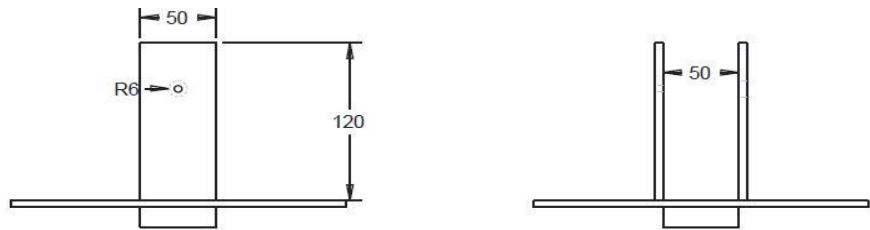


Figure 3.8: Block Diagram of the System

2D designs and dimensions:

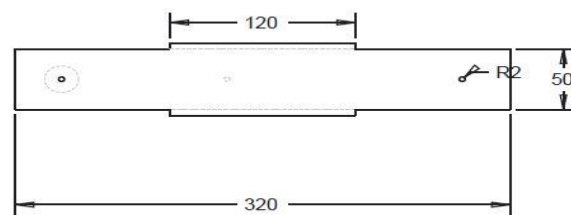
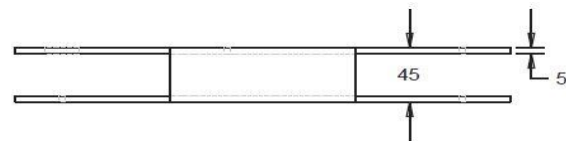
The following are the 2D drawings of the various parts of the manipulator.

All dimensions are in mm.



Link 1

Figure 3.9: Link1 – Base link with the movable platform.



Link 2

Figure 3.10: Link2 – The link with the pulley assembly

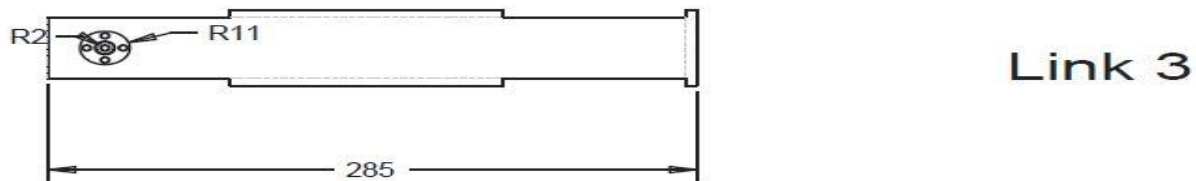
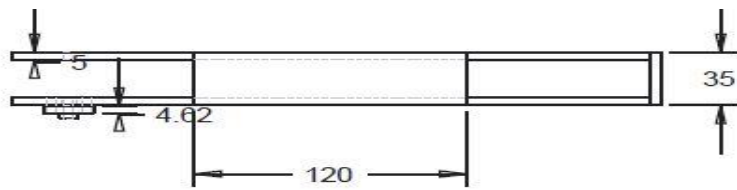


Figure 3.11: Link 3

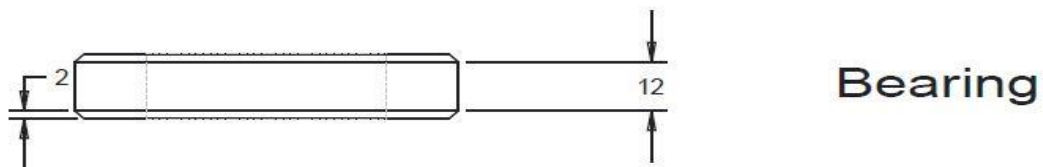
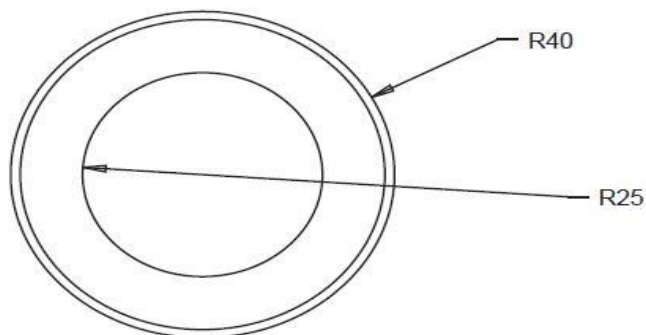


Figure 3.12: Bearing – press fitted on the moving platform.

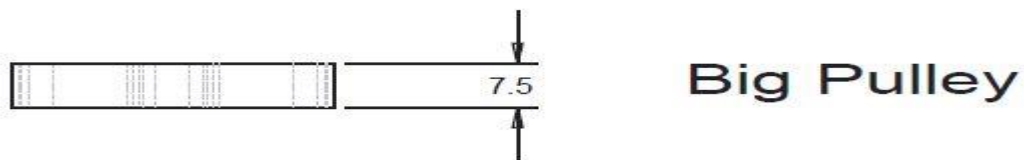
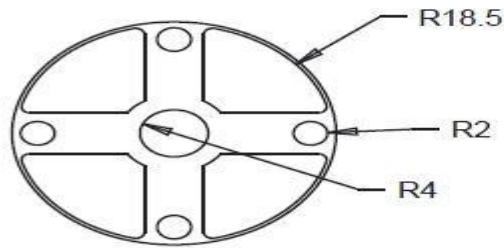
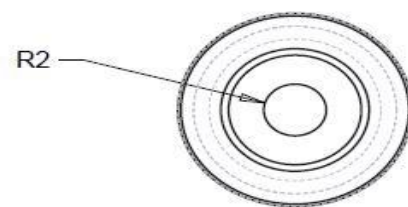
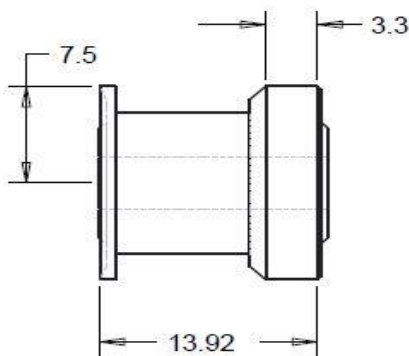


Figure 3.13: Big Pulley



Small Pulley

Figure 3.14: Small Pulley

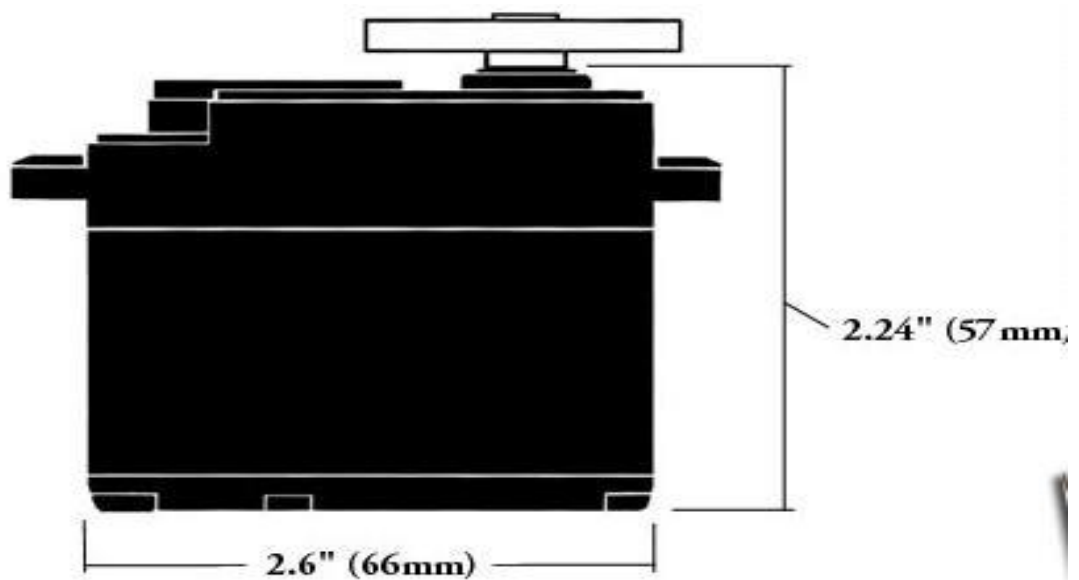


Figure 3.15: Servomotor HS-805MG

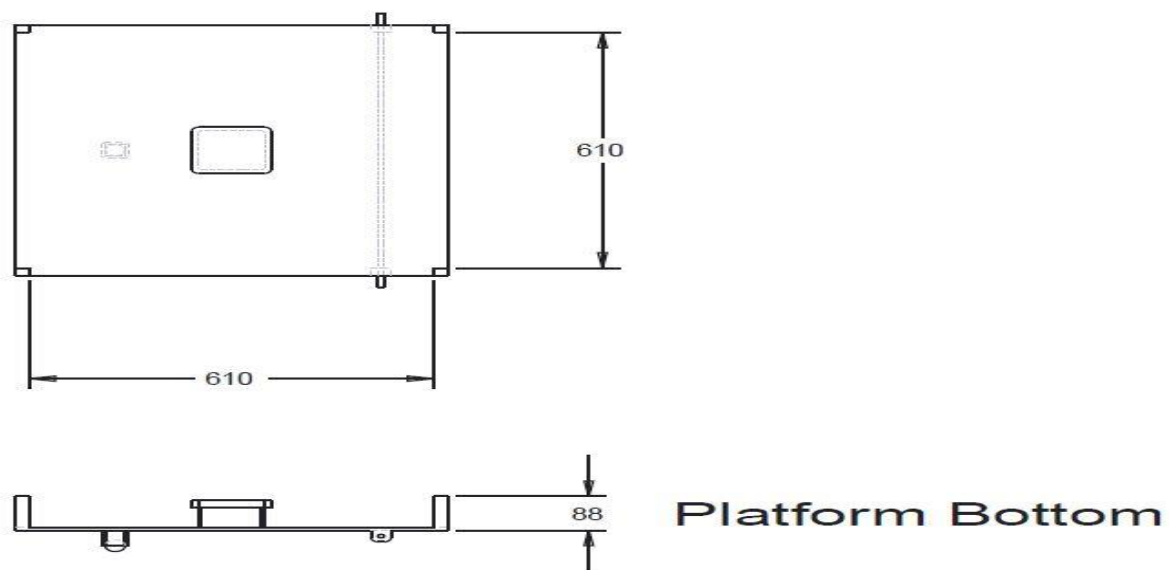


Figure 3.16: Platform – Bottom Half

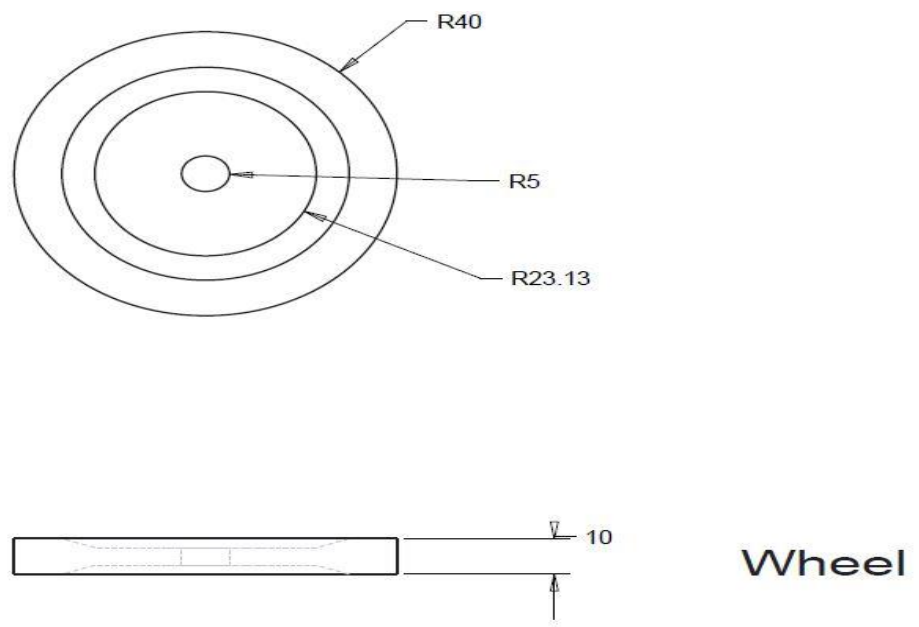


Figure 3.17: Robot Wheels

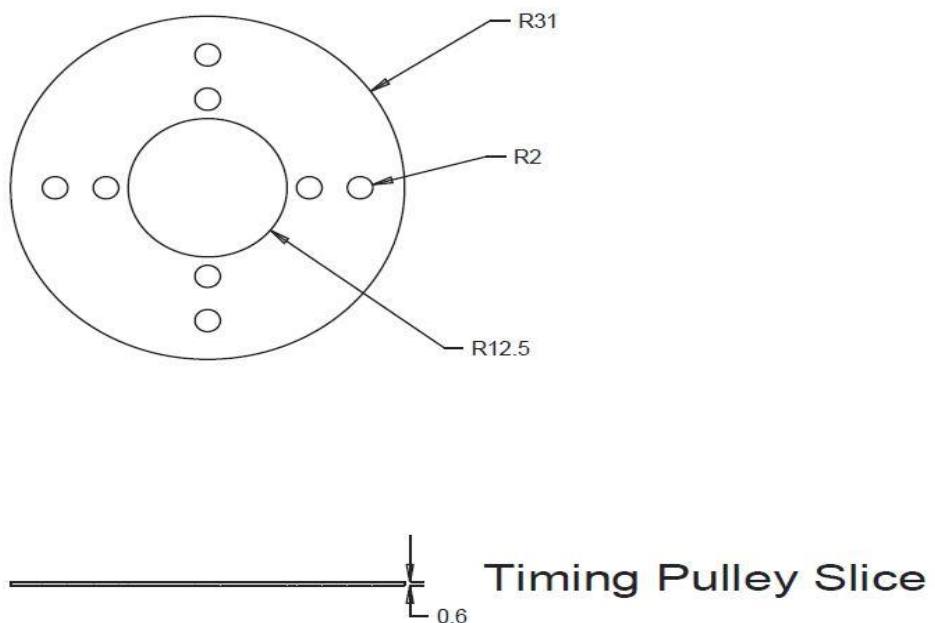


Figure 3.18: Timing Pulley Slice

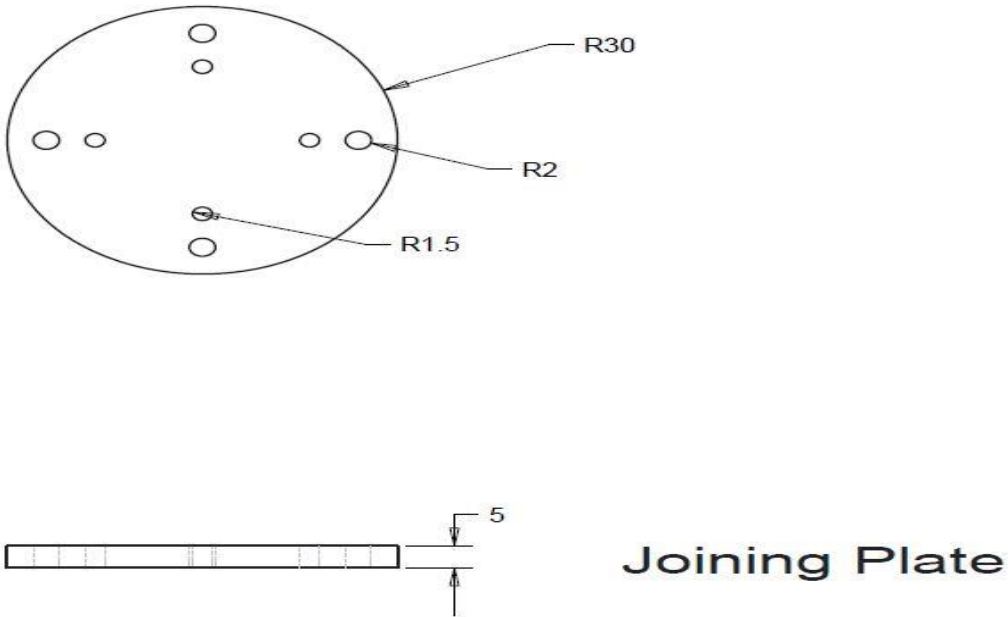


Figure 3.19: Joining Plate (Acrylic) – Specifically made for the proper mounting of the pulley and motor.

Joint Angle Range:

The following is the max range of the angles (based on geometric or motor constraints) that could be achieved by each joint.

JOINTS	TORQUE RATINGS	ANGLE RANGE
Joint 1	23.9Kg-cm	0 to 180deg.
Joint 2	23.9Kg-cm	-70 to +90deg.
Joint 3	23.9Kg-cm	-90 to +90deg.

Table 3.1: Joint Angle Range

Forward Kinematics

Firstly we perform frame allocation on our 3 DOF arm. For this we first put the arm in its ‘home position’ and then follow the frame allocation rules.

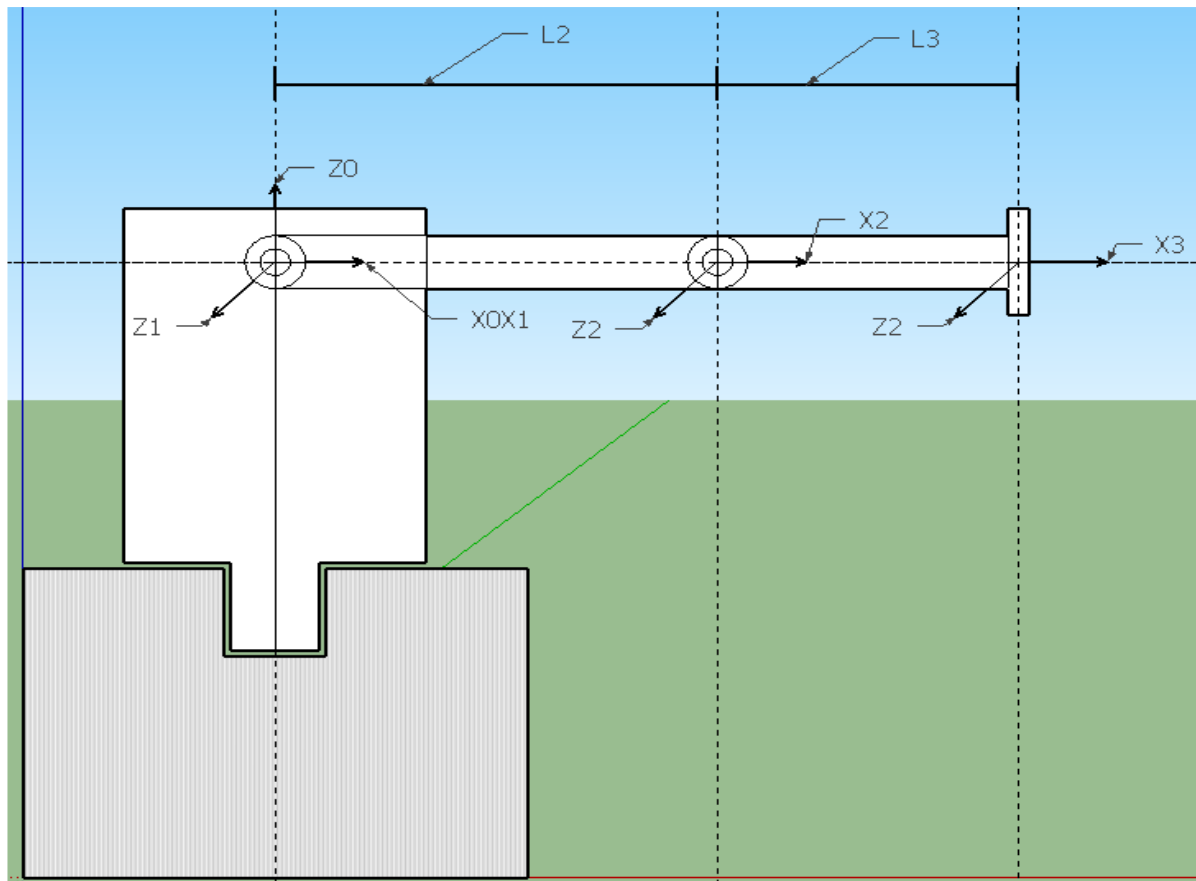


Figure 3.20: Frame Allocation on the joints.

Now as the frames are allotted, we find out the values of the ‘dh parameters’ for each link.

The D-H Parameters are:

LINK i	1	2	3
a_i	0	$L_2=259.08\text{mm}$	$L_3=255\text{mm}$
α_i	+90deg	0deg	0deg
d_i	0	0	0
θ_i	Θ_1	Θ_2	Θ_3

Table 3.2: Values of d-h parameters for the arm

Using

$${}^{i-1}\mathbf{T}_i = \begin{bmatrix} C\theta_i & -S\theta_i C\alpha_i & S\theta_i S\alpha_i & a_i C\theta_i \\ S\theta_i & C\theta_i C\alpha_i & -C\theta_i S\alpha_i & a_i S\theta_i \\ 0 & S\alpha_i & C\alpha_i & d_i \\ 0 & 0 & 0 & 1 \end{bmatrix}$$

We find the homogeneous transformation matrices

$$\mathbf{T}_1^0(\theta_1) = \begin{bmatrix} c_1 & 0 & s_1 & 0 \\ s_1 & 0 & -c_1 & 0 \\ 0 & 1 & 0 & 0 \\ 0 & 0 & 0 & 1 \end{bmatrix} \quad \mathbf{T}_2^1(\theta_2) = \begin{bmatrix} c_2 & -s_2 & 0 & l_2 c_2 \\ s_2 & c_2 & 0 & l_2 s_2 \\ 0 & 0 & 1 & 0 \\ 0 & 0 & 0 & 1 \end{bmatrix} \quad \mathbf{T}_3^2(\theta_3) = \begin{bmatrix} c_3 & -s_3 & 0 & l_3 c_3 \\ s_3 & c_3 & 0 & l_3 s_3 \\ 0 & 0 & 1 & 0 \\ 0 & 0 & 0 & 1 \end{bmatrix}$$

*The value of L_1 and L_2 are noted in the dh table and the overall matrix.

Thus we get the overall transformation matrix as

$$\mathbf{T}_3^0 = \begin{bmatrix} c_1 c_{23} & -c_1 s_{23} & s_1 & c_1 [255 c_{23} + 259.08 c_2] \\ s_1 c_{23} & s_1 s_{23} & -c_1 & s_1 [255 c_{23} + 259.08 c_2] \\ s_{23} & c_{23} & 0 & [255 s_{23} + 259.08 s_2] \\ 0 & 0 & 0 & 1 \end{bmatrix}$$

*Where $S_{23} = \sin(\theta_2 + \theta_3)$ and $C_{23} = \cos(\theta_2 + \theta_3)$, $C_1 = \cos(\theta_1)$, $S_1 = \sin(\theta_1)$

Inverse Kinematics:

Inverse Kinematics:

We used ‘closed form solution technique’ in order to perform inverse kinematics so as to find out the joint angles when position and orientation of gripper is known.

The known position and orientation of the endpoint of arm can be denoted by

$$\begin{bmatrix} r_{11} & r_{12} & r_{13} & r_{14} \\ r_{21} & r_{22} & r_{23} & r_{24} \\ r_{31} & r_{32} & r_{33} & r_{34} \\ 0 & 0 & 0 & 1 \end{bmatrix}$$

These values are either constants or zeros.

So now we equate our transformation matrix and the above known position and solve it for θ_1 , θ_2 and θ_3 .

$$\begin{bmatrix} C_1C_{23} & -C_1S_{23} & -S_1 & C_1(255C_{23} + 259.08C_2) \\ S_1C_{23} & -S_1S_{23} & C_1 & S_1(255C_{23} + 259.08C_2) \\ S_{23} & C_{23} & 0 & 255S_{23} + 259.08S_2 \\ 0 & 0 & 0 & 1 \end{bmatrix} = \begin{bmatrix} r_{11} & r_{12} & r_{13} & r_{14} \\ r_{21} & r_{22} & r_{23} & r_{24} \\ r_{31} & r_{32} & r_{33} & r_{34} \\ 0 & 0 & 0 & 1 \end{bmatrix}$$

Solution for θ_1 :

Observing the above matrices we find that element (1,4) and element (2,4) of both have only θ_1 as variable. Thus we get

$$S_1/C_1 = r_{24}/r_{14}$$

Thus $\theta_1 = \text{Atan2}(r_{24}, r_{14})$

Solution for θ_2 and θ_3 :

For θ_2

These joint angles cannot be directly found so we use the inverse transformation approach to find them.

$${}^0T_1 {}^1T_2 {}^2T_3 = {}^0T_3$$

So we first separate θ_2 from θ_3 .

$${}^0T_1 {}^1T_2 = {}^0T_3 [{}^2T_3]^{-1}$$

$$\begin{bmatrix} C1C2 & -C1S2 & S1 & 259, .08C1C2 \\ S1C2 & -S1S2 & -C1 & 259.08S1C2 \\ S2 & C2 & 0 & 259.08S2 \\ 0 & 0 & 0 & 1 \end{bmatrix} =$$

$$\begin{bmatrix} C3r11 - S3r12 & S3r11 + C3r12 & r13 & -255r11 + r14 \\ C3r21 - S3r22 & S3r21 - S3r22 & r23 & -255r21 + r24 \\ C3r31 - S3r32 & S3r31 - S3r32 & r32 & -255r31 + r34 \\ 0 & 0 & 0 & 1 \end{bmatrix}$$

By squaring and adding elements (1,4) and (2,4) we get

$$259.08*C2 = (+/-) [(-255*r11+r14)^2 + (-255*r21+r24)^2]^{1/2}$$

We divide this obtained equation by element (3,4)

$$\theta_2 = \text{Atan2} [(-255*r31+r34), (+/-) [(-255*r11+r14)^2 + (-255*r21+r24)^2]^{1/2}]$$

For θ_3

We use $S23 = r31$ and $C23 = r32$ (From original equation).

$$S23/C23 = r31/r32$$

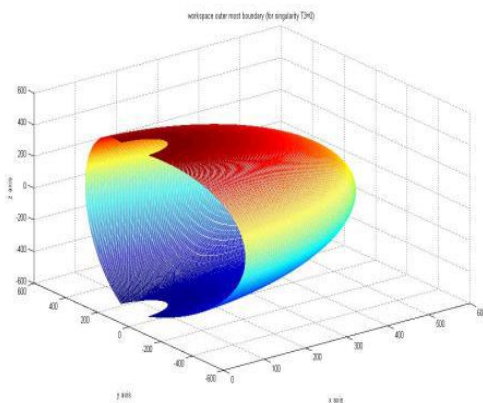
$$\theta_2 + \theta_3 = \text{Atan2}(r31, r32).$$

Thus from the known positions of the end effector, the joint angles can be found out from the above equations.

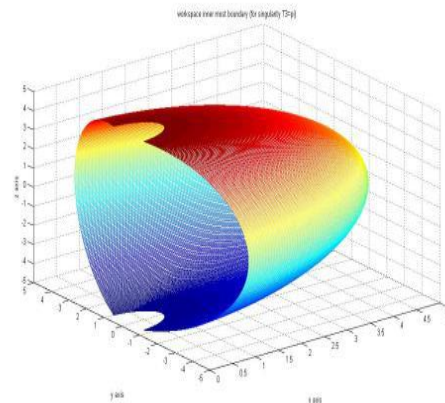
Singularities:

Singularity is defined as “a condition caused by the collinear alignment of two or more robot axes resulting in unpredictable robot motion and velocities.” The result of a singularity can be quite dramatic and can have adverse effects on the robot arm, the end effector, and the process. Some industrial robot manufacturers have attempted to side-step the situation by slightly altering the robot’s path to prevent this condition. But in order to alter the robot’s path, one first needs to know where these singularity positions actually are. So we created the Workspace plot of our robot using Mat Lab.

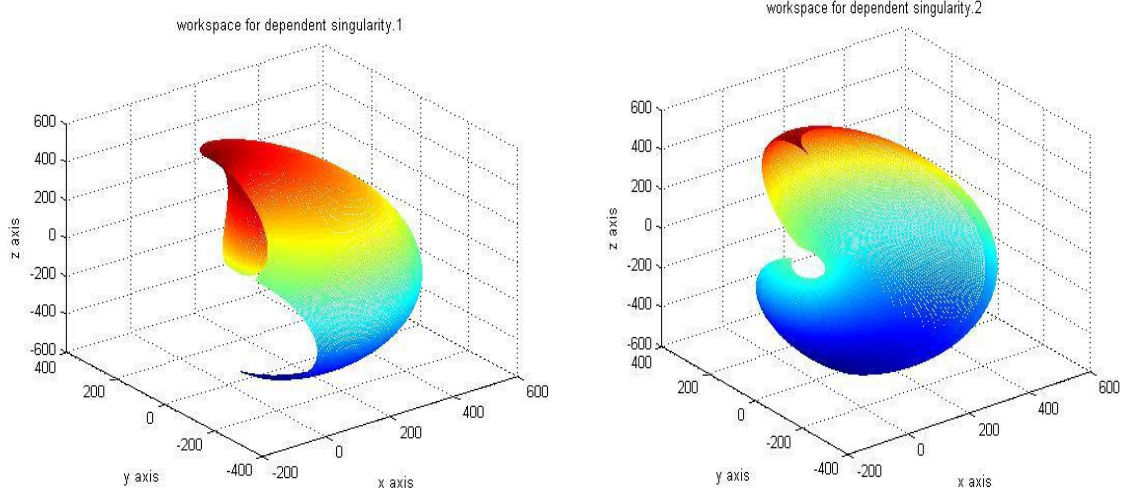
Workspace and singular configurations



Singularity Condition $\theta_3=0$



Singularity Condition $\theta_3 = \pi$

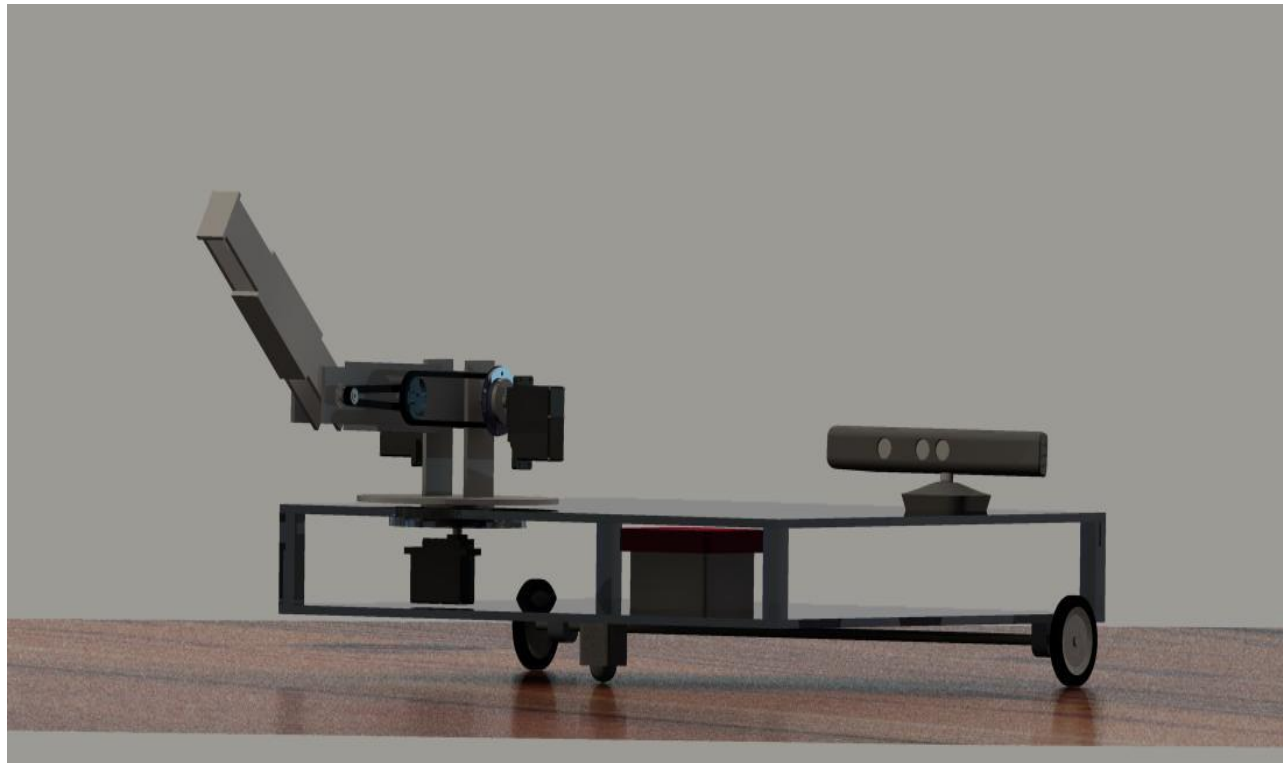


Singularity Condition $L2C2 + L3C23 = 0$

Singularity Condition $L2C2 + L3C23 = 0$

Figure 3.21: Different singularity conditions observed by the arm.

Final CAD (CREO) Model:



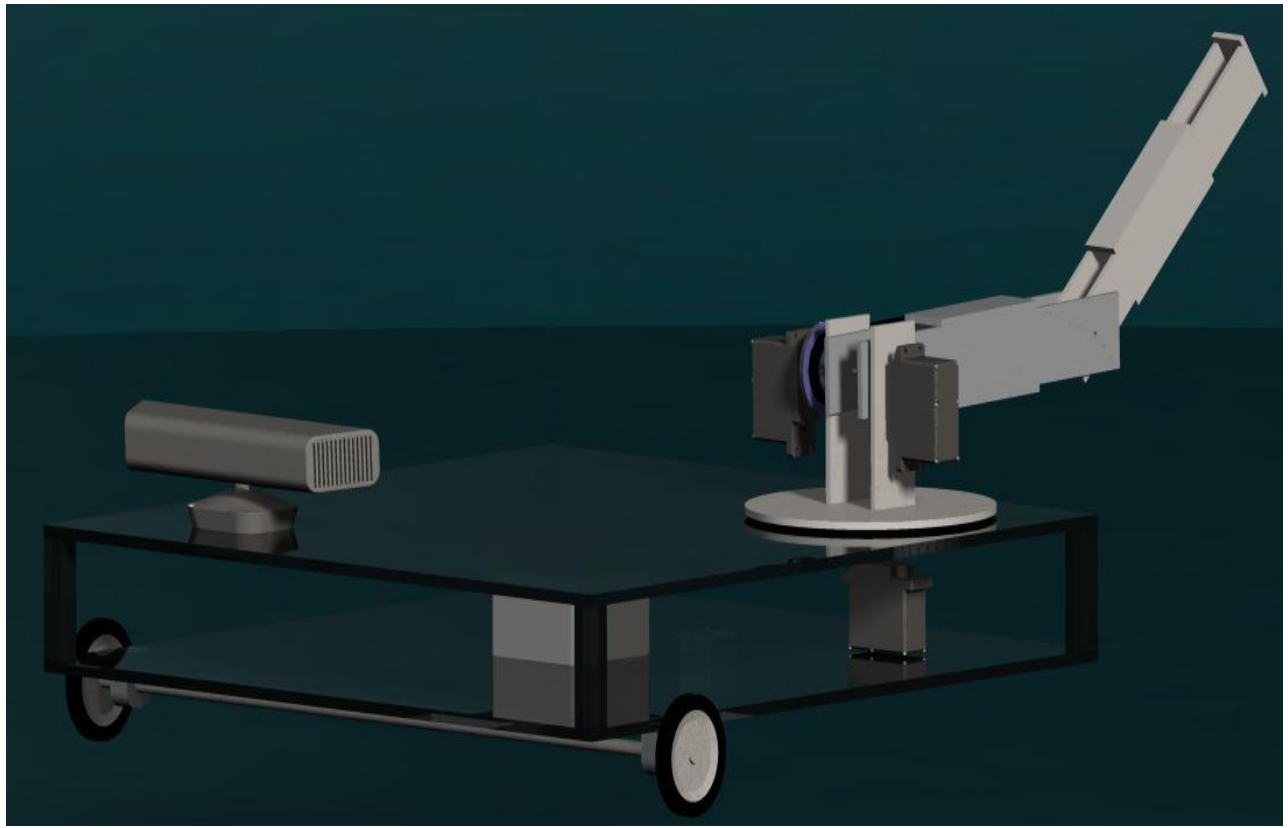


Figure 3.22: Final CAD Model

4 ROBOTIC GRIPPER

4.1 INDEX

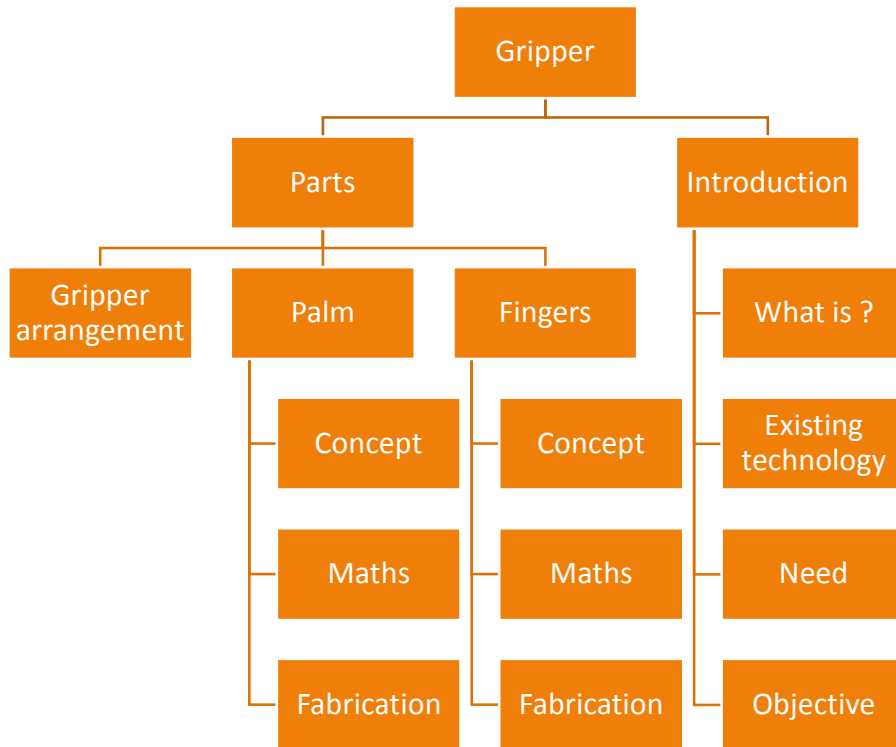


Figure 4.1: Index for gripper

4.2 INTRODUCTION

4.2.1 What is a Gripper or End effector?

A robot gripper is a type of end of arm tooling (EOAT) that is used to pick up items and can be customized for your application.

In robotics, an end effector is the device at the end of a robotic arm, designed to interact with the environment. The exact nature of this device depends on the application of the robot.

4.2.2 Existing technology

End effectors may consist of a gripper or a tool. When referring to robotic prehension there are four general categories of robot grippers, these are

1. Impactive – jaws or claws which physically grasp by direct impact upon the object.
2. Ingressive – pins, needles or hackles which physically penetrate the surface of the object (used in textile, carbon and glass fiber handling).
3. Astrictive – suction [vague] forces applied to the objects surface (whether by vacuum, magneto- or electro-adhesion).
4. Contigutive – requiring direct contact for adhesion to take place (such as glue, surface tension or freezing).

The most known mechanical gripper can be of two, three or even five fingers.

4.3 THE GRIPPER

4.3.1 The arrangement

Of all the above mentioned existing gripper designs, the prospective base designs were narrowed down to impactive type grippers, due to its flexibility, unlike the other 3 major types of grippers which appeal to very specific types of applications. Objects encountered in industries may be vaguely generalized to be rigid, solid shapes that resemble or constitute common 3D shapes as a base templates or discrete parts respectively.

The prospective systems for power transmission in grippers were as follows:

1. Mechanical :
 - a. Gears
 - b. Linkages
2. Pneumatic
3. Hydraulic
4. Vacuum

The second criterion for selection for selection of gripper base model, was contact type. Common contact surfaces include:

1. Suction cups

2. Fingers:

a. 2

b. 3

c. 3+

4.3.2 Comparison gripper base model's parameters

Parameters	Mechanical	Pneumatic	Hydraulic
Power	3	3	5
Cost effectiveness	5	3	1
Portability	5	2	2
Total	13	8	8

Table 4.1: Comparison between grippers based on type of input energy for gripping

Parameters	2 Finger	Concentric 3 Finger	3+ fingers	Vacuum cups
Cost effectiveness	5	4	3	3
Smooth surface handling	3	4	5	5
Rough surface handling	5	5	5	2
Ease of programming	5	4	2	5
Parallel surface handling	5	3	5	5
Curved surface handling	1	5	5	3
Redundancy for application(lack of)	5	4	0	2
Total	29	29	25	25

Table 4.2: Comparison between grippers based on no. of fingers or their placements

4.3.3 Summary and conclusion

In context of the problem statement, mechanical linkages and gears prove to be the superior choices for the gripper's base model. With respect to the contact surfaces, 2 & 3 finger contact, both prove to be in close contention. However, we can notice that both excel in different avenues, with one showing great results where the other fails miserably. 2 finger mechanisms excel at handling parallel surfaces,

while 3 finger mechanisms impress at handling curved surfaces and countering moments, if the gripping position is off center of gravity.

In their basic form neither 2 finger nor 3 finger grippers show sufficient flexibility for gripping a majority of standard shapes. The need for a unique & unconventional design using gears & mechanical linkages was apparent.

4.3.4 Design considerations

1. Minimization of No. of motors.
2. Maximization of flexibility.
3. Maximizing torque utilization.

4.3.5 Base Schematic

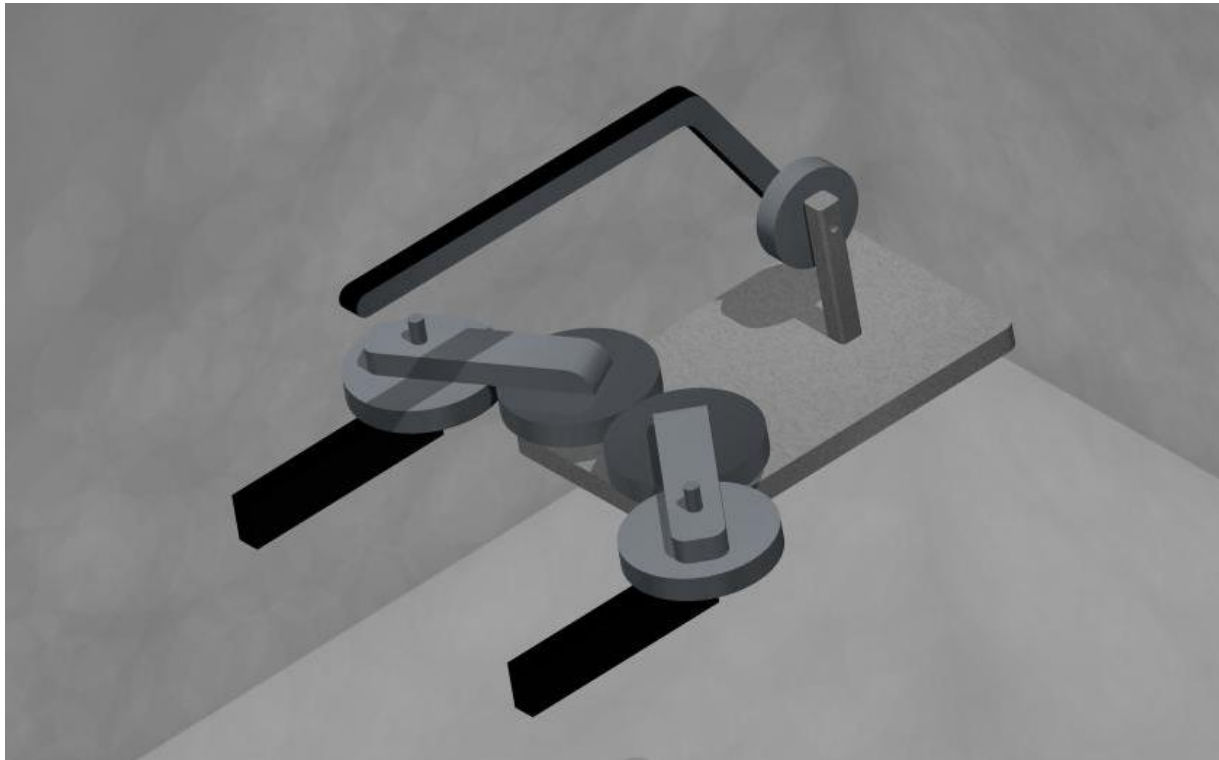


Figure 4.2: Gripper (Earlier Design) – Basic Diagram with gears.

4.3.6 Advantages over standard designs:

The schematic design visualized above incorporates strengths from both standard 2 & 3 finger grippers. 2 horizontal fingers provide gripping in the horizontal plane while functioning as a standard 2 finger gripper.

The 3rd finger provides support to counter stray moment incorporated due to off center gripping.

This design provides the flexibility and robustness of a 3+ (usually 5) finger gripper while being compact, simple, cost effective and much less redundant.

4.3.7 Final render:



Figure 4.3: Gripper (Final Design) – With parallel link mechanism

4.4 THE PALM:

The palm of the gripper, refers to gear & mechanical linkage network used to transmit

4.4.1 Concept:

For horizontal gripping, the objective was to design a mechanism using gears and linkages that would enable parallel gripping. Parallel gripping has multiple advantages over simple angular gripping, as it avoids accidental slipping and ensures force applied is along a single axis, as opposed to angular gripping where the direction of force changes for each probable position.

Torque transmission takes place from the servo to the linkages to the finger which then comes in contact with the object to be handled. It is also imperative that the 2 fingers move in opposite directions, in the same velocity and close perfectly at one extreme position. For this, the following gear arrangement is utilized.

THE GEAR ARRANGEMENT

The gears are connected to a link, that pushes another link that forms a part of a 4 bar mechanism. The 4 bar mechanism ensures parallel movement of the gripper surface and amplification of the smaller displacement of gear to the desired opening of the jaw.

4.4.2 Mathematical modelling

Shown Below are schematics highlighting the various variables and constraints that are to be defined and controlled in the designing of the gripper's palm.

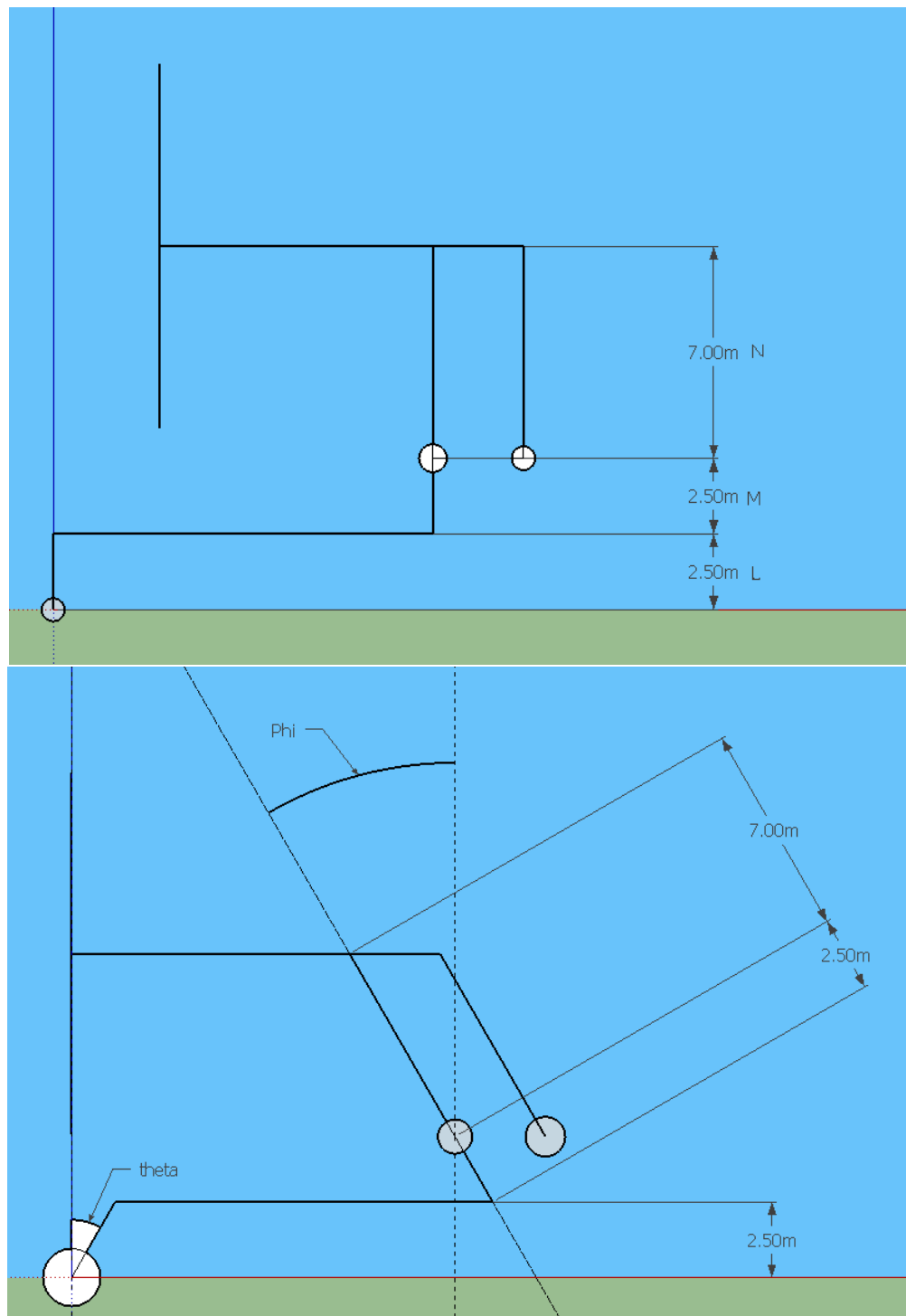


Figure 4.4: Mathematical Diagram of gripper

Selection of co-efficient of friction:

Material-1	Material-2	Co-efficient of friction
Brake material	Cl	0.4
Cl	Cl	0.51
Cl	Steel	0.4
Leather	Metal	0.61
Leather	Wood	0.61

Table 4.3: Coefficient of friction between different materials

Assume $\mu_{\text{minimum}} = 0.3$ (From above values)

Assume Mass = m = 100 grams (Design constraint)

Max deflection for 1 arm = 7 cm (Design constraint)

$$T = \frac{0.1}{0.3} * N * \frac{L}{M} * \frac{1}{\cos(\theta)} * \frac{1}{(\cos(\varphi))^2}$$

$$X = \frac{2 * N * \sin(\theta) * L}{M}$$

$$L * \sin \theta = M * \cos \varphi$$

In the above equations:

T: Input torque

L, M, N: Link lengths as shown in schematic

θ, φ : Angles for link rotation as shown in schematic

X: Deflection of jaw in one direction

Since the number of variables is more than the number of equations

The following considerations were made:

1. L/M is assumed to be one variable
2. $\theta_{\text{maximum}} = 30 \text{ degrees}$
3. L = M

Solving, we get:

$$L = M = 2.5 \text{ cm}$$

$$N = 7 \text{ cm}$$

$$T = 3.5 \text{ kg/cm}$$

Taking factor of safety into consideration, a servo for 5 kg/cm torque would be appropriate.

4.5 THE FINGERS

4.5.1 Concept:

The ends of the jaw, which come in contact with the object to be picked up are referred to as the fingers of the gripper.

Conventionally, contact is established using either a rigid surface as in 2 finger grippers or spherical points as in concentric 3 finger grippers. However, contact in each case is merely point contact and force is transmitted only at those 2 or 3 points. This means that should the object be of an unconventional shape, the fingers might be unable to reliably grip the object or restrict its motion along a perpendicular axis.

Having multiple points of contact, where each normal reaction is in a different direction, ensures that such a gripper will have a much lower number of unconventional objects that it might have trouble handling.

Such a gripper however, needs to be adaptive, such that it recognizes when simple point contact would be suitable while adapting to scenarios where multiple points of contact might be appropriate.

In accordance with these considerations, the following design has been visualized.

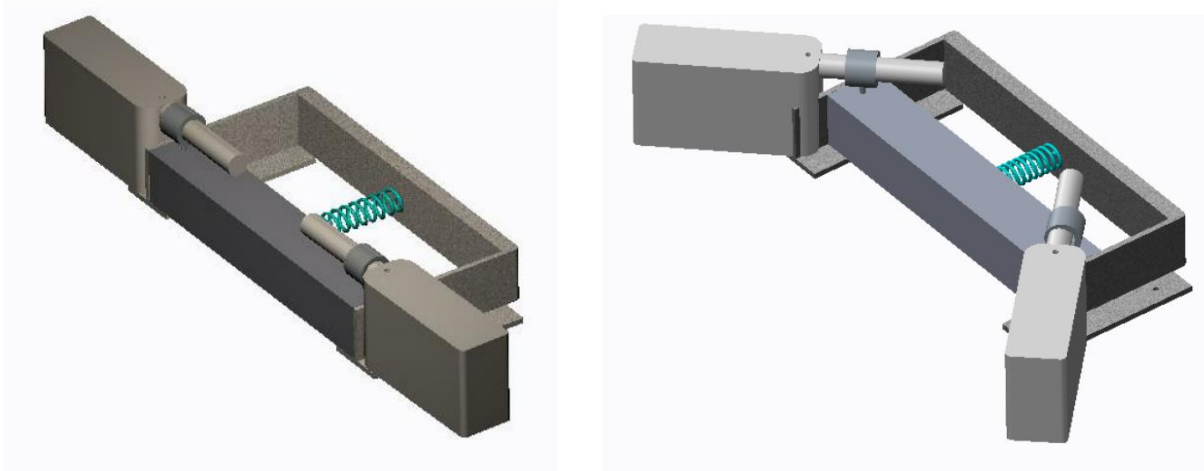


Figure 4.5: Working diagram of the finger in different positions

The finger is split into 3 parts, out of which 2 are symmetrical. The arrangement is such that when initial contact is made with the central part, it is displaced and the spring undergoes compression. The displacement of the central sub-finger cause the rotation of the other 2 parts about a pivot, due to sliding of the cylindrical extension through the sliding and swivel joint attached to the central contact surface.

The mechanism obtains equilibrium when the outer contact surfaces come in contact with the object to be gripped, thus establishing multi point contact.

4.5.2 Mathematical modelling

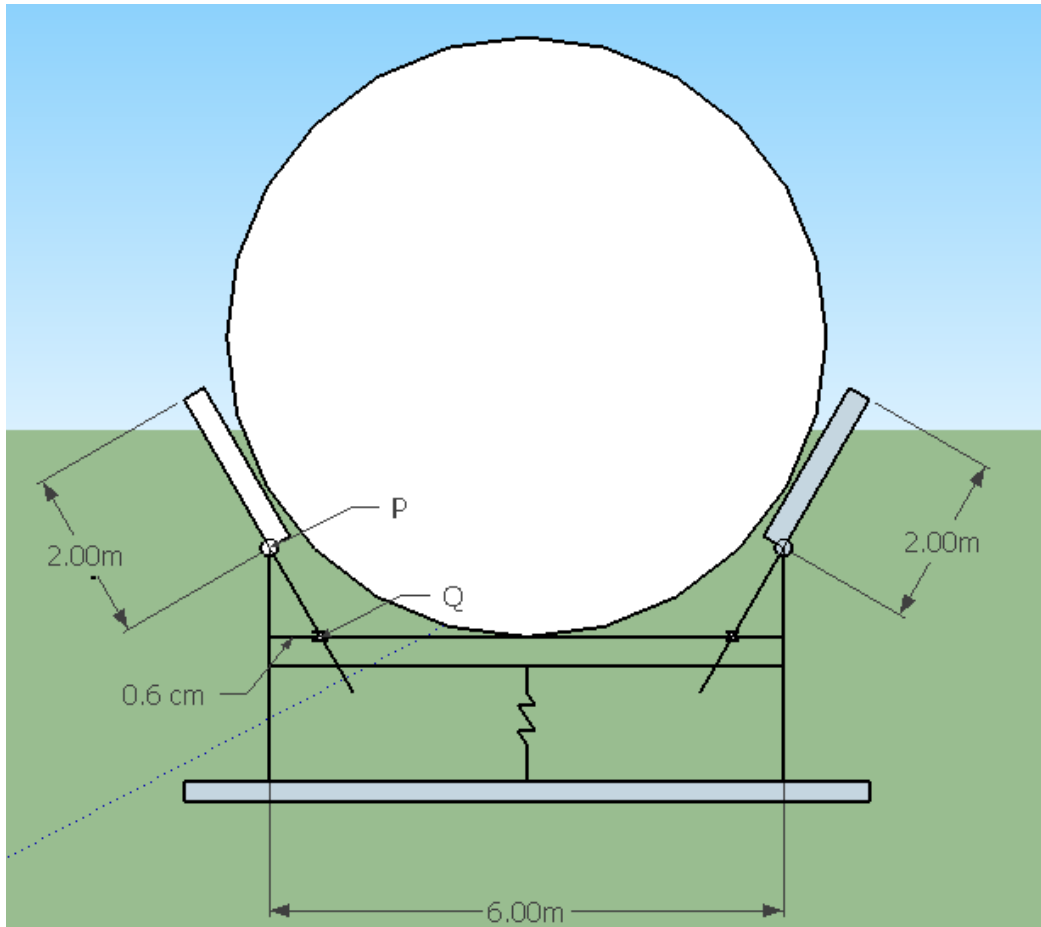


Figure 4.6: Schematic diagram showing gripper grabbing a spherical object.

Above is a schematic showing a curved object being gripped by the gripper finger.

Using geometrical relations we get the following equations:

$$\tan(\theta) = \frac{D - A}{R}$$

$$B + C = D - A$$

$$E \geq B$$

$$\cos(\theta) = \frac{A}{C}$$

Here,

ϕ : Angle rotated by outer contact surfaces

A: Dist. PQ when at rest

B: Dist. From tangent to Q

C: Distance PQ after maximum rotation

D: Length of central contact surface

R: Radius of smallest circle to be gripped

5 FABRICATION

The fabrication of the robot was divided into three main parts, namely, the mobile platform, the robotic arm and the gripper.

5.1 MOBILE PLATFORM

The mobile platform's function, as its name suggests, was to provide mobility to the robot. Any moving object should have sufficient contact points with the ground so that its orientation with respect to the ground remains same at all times during the operation. Hence, a four-wheeled platform was found to be appropriate for use. This platform had to take the robotic arm to the required location with precision. So, it is driven by encoder motors which provide accurate motion to the wheels. Two castor wheels are provided in the front of the platform for the ease of direction ability.

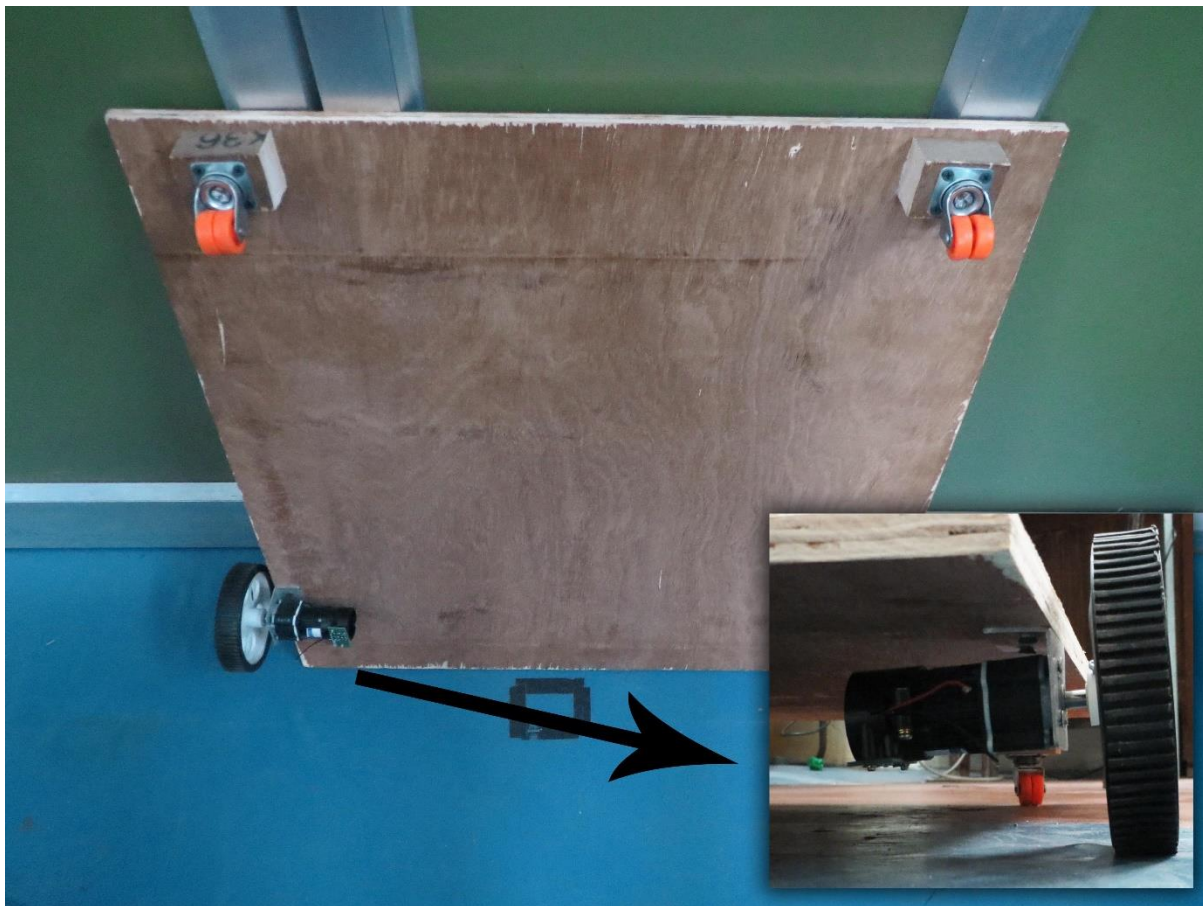


Figure 5.1: Depicts arrangement of wheel and encoder motors at the bottom of the moving platform.

Working with a Kinect camera adds some constraints to the design and fabrication of an assembly as Kinect can detect an object only if it is more than 400 mm away from it. Also, nothing should be in its viewing angle, horizontal or vertical. Based on this constraints, the size of the platform was decided to be 650mm*650mm. The platform is made of wood so as to keep it light and wheels and encoder motors were attached to it at the back with suitable arrangement. Based on the height of the platform attained due to the wheels at the back, the castor wheels on the front were fitted so as to keep the platform horizontal with respect to the ground.

5.2 ROBOTIC ARM

As the design showed that the arm had three joints, three motors were thus required, one to actuate each joint. The first motion that was to be provided to the arm was the rotation of the first link. As this joint will be subjected to load equivalent to the weight of the arm, special care had to be taken to design and fabricate it. It was decided to use a bearing for providing a joint as frictionless as possible. An arrangement as shown in the figure was made which provided the required support for the arm and the bearing.

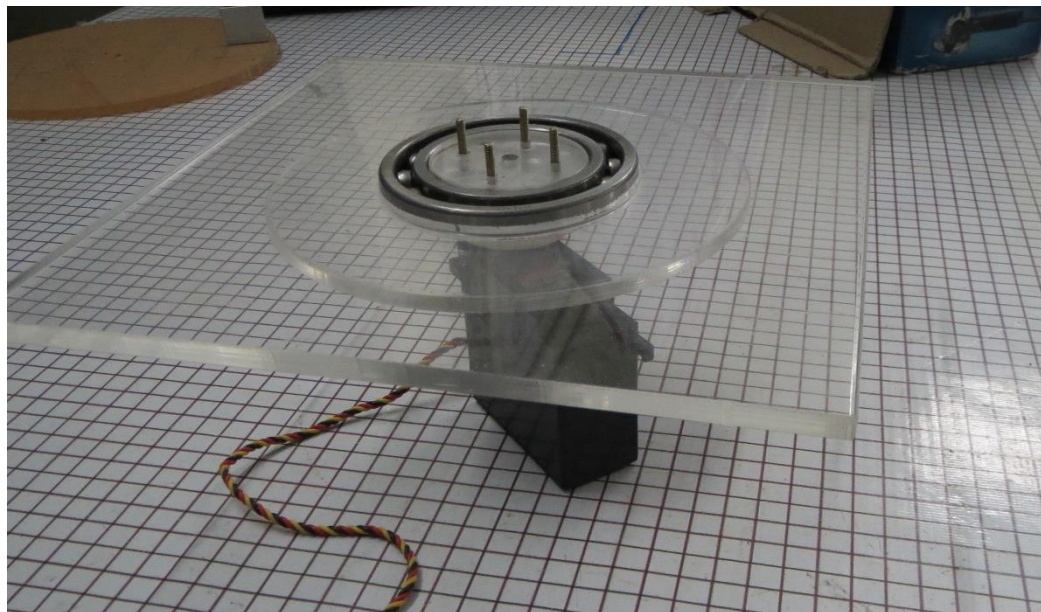


Figure 5.2: Shows motor to be placed on the platform with movable platform arrangement.

The acrylic plates which do not have any relative motion between them are stacked together using proper adhesives and the bearing was manually press-fitted into its housing.

Now comes the first link of the arm and the two motors which are to be fixed with respect to the rotating platform. An extensive arrangement using aluminium angles was used to accomplish this task because they provide the required stiffness and the included right angle with which the requirements can be met with ease.



Figure 5.3: Arm assembly (without platform and gripper)

The second motor which drives the second link of arm is directly connected to it with an attachment as shown in the picture.

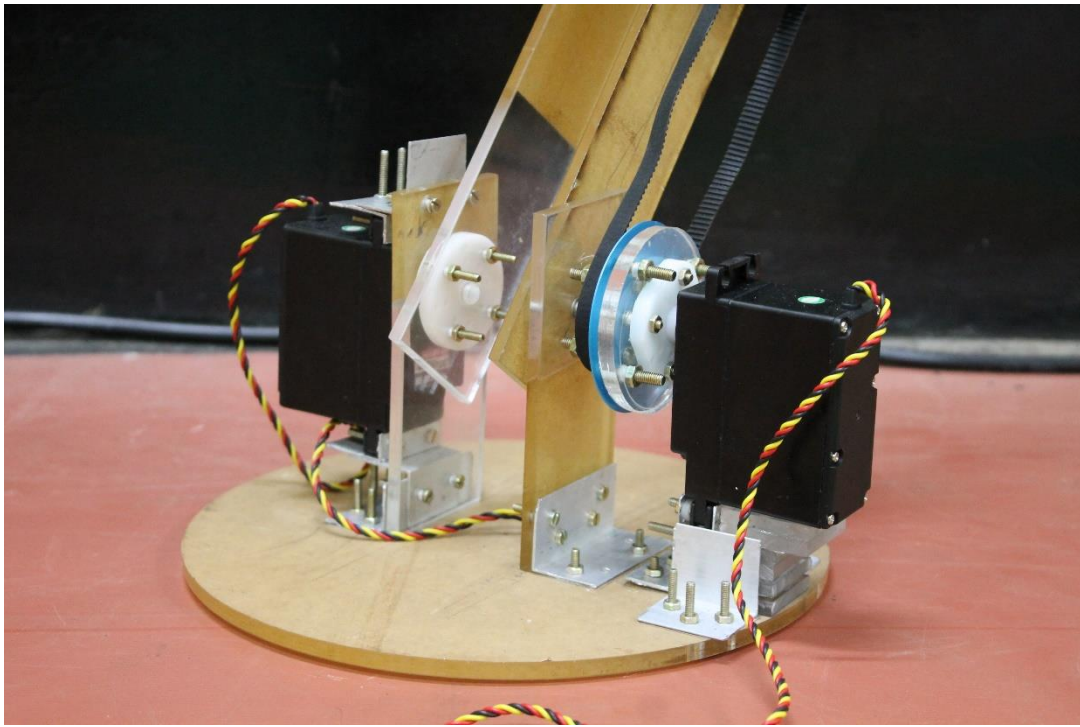


Figure 5.4: Placement of 2nd and 3rd motor with aluminium angles

Now, the third motor which actuates the third link of arm is also kept on the rotating base and hence to transmit the rotational motion from motor to the link, a timing belt drive was devised. Timing belts are used because they provide precise motion transmission and no slip conditions. Due to unavailability of the belt size which were required, two small belts were used in such an arrangement so that the speed ratio remains 1:1 and the required length is also achieved.

The first belt drive transmits power from the motor shaft to the intermediate shaft. The attachment between motor and the timing belt pulley are custom made so as to fit properly.

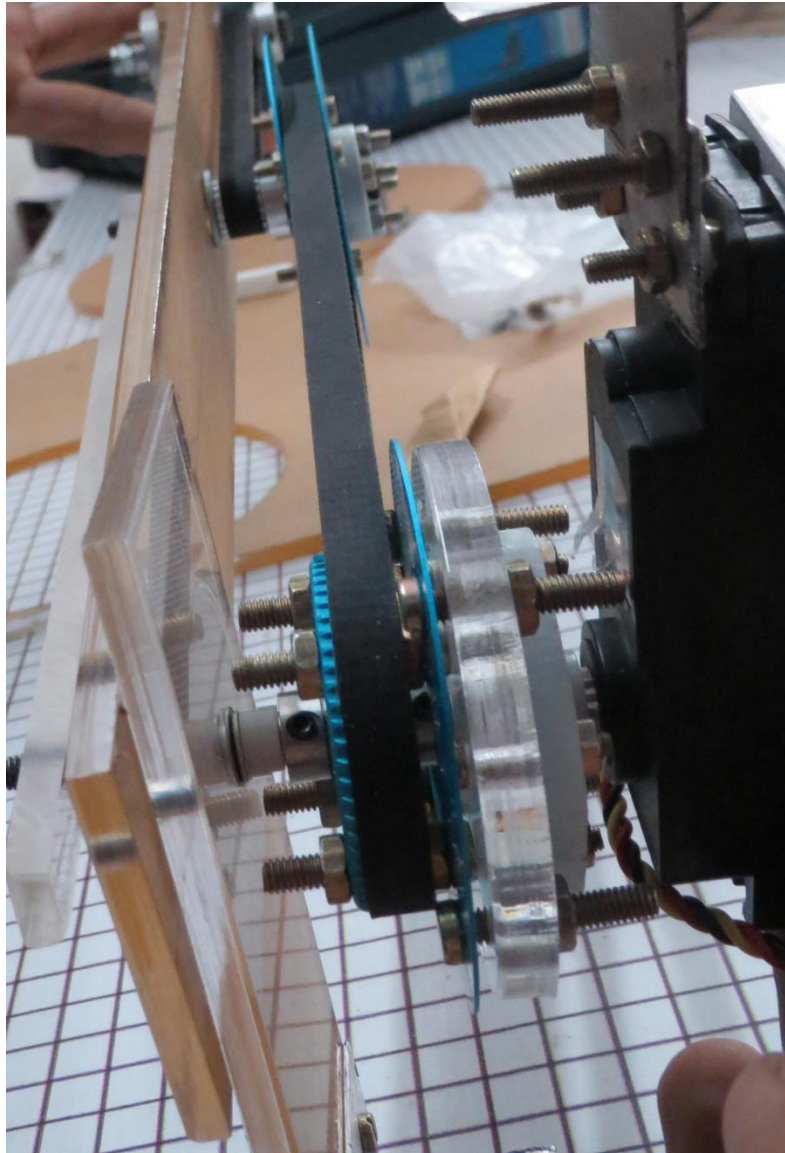


Figure 5.5: Arrangement of timing pulleys and belts to drive the 3rd joint by 3rd motor placed at the 2nd Joint.

The intermediate shaft contains two pulleys which resemble a compound pulley arrangement. This shaft is fixed into the second link. This shaft does not directly contribute to the motion of the third link, it just transmits power from 1st belt drive to the 2nd belt drive. In this arrangement, both the pulleys and the shaft are not allowed to have to have any relative motion between them. This is ensured with the help of 'grub' screws.

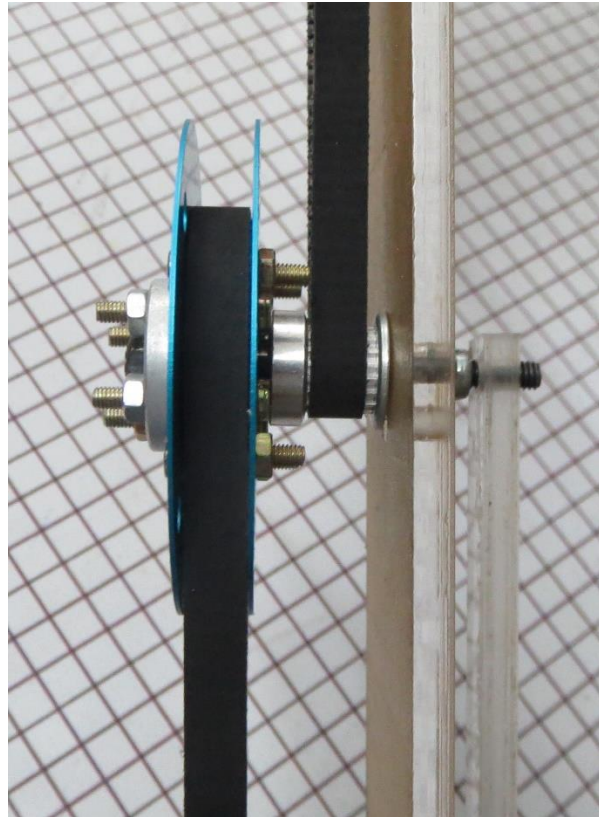


Figure 5.6: Power transmission from 1st belt to the 2nd

The final shaft contains a pulley and an attachment for driving the 3rd link.

5.3 THE GRIPPER

As the gripper is to be attached to the 3rd link of the arm, its weight is a matter of very serious concern. Each gram increase in its weight would have a multiplied effect on the motors on the rotating base. Hence, it was of utmost importance that the gripper and finger mechanism to be made from a material which is light but provides sufficient amount of strength. Hence all the linkages and components of gripper and finger mechanisms were made in a 3-D printer which uses PLA plastic and whose 'infill density' can be varied according to the size of the component and the strength required.

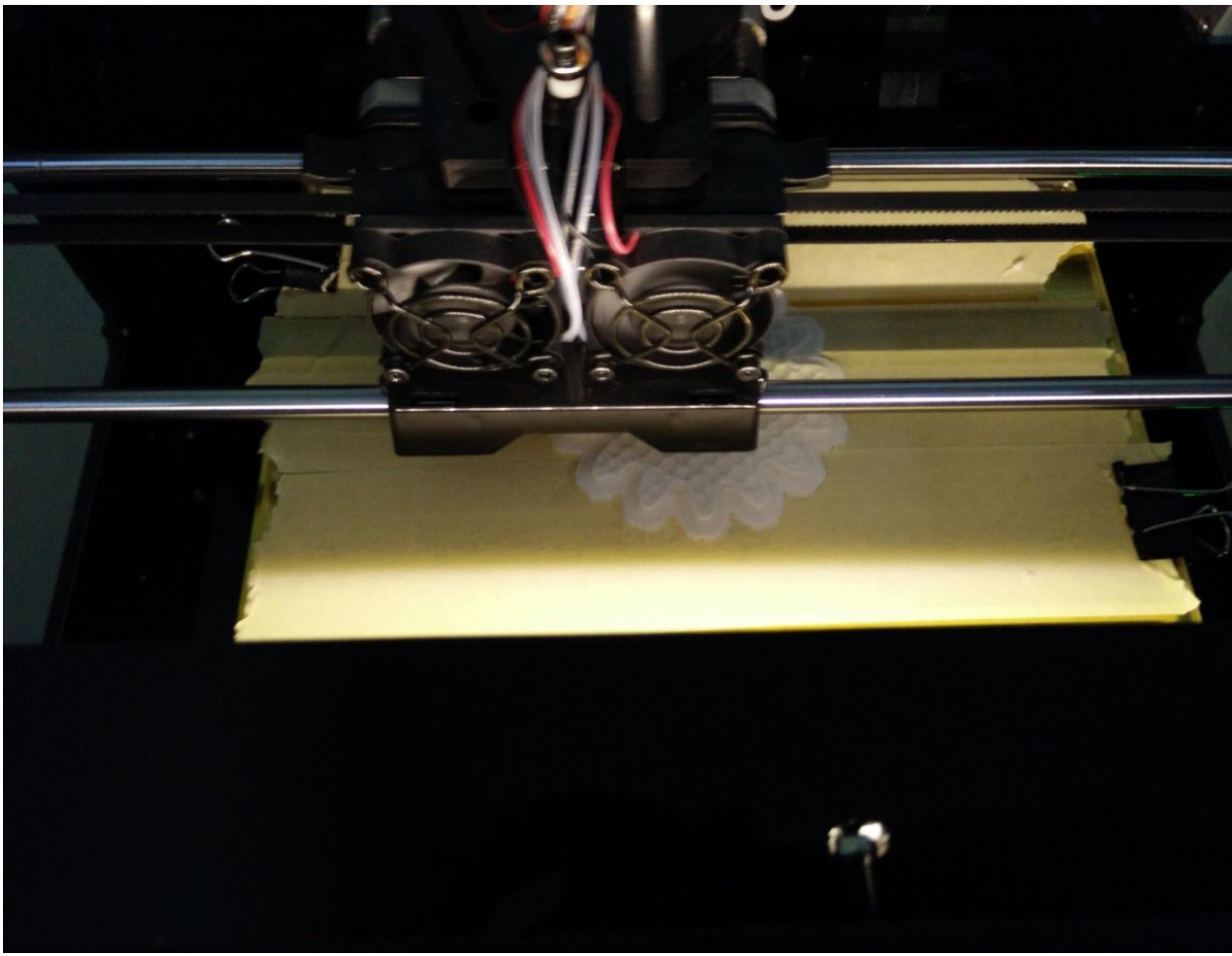


Figure 5.7: A gear being made by the 3D printer – PLA plastic

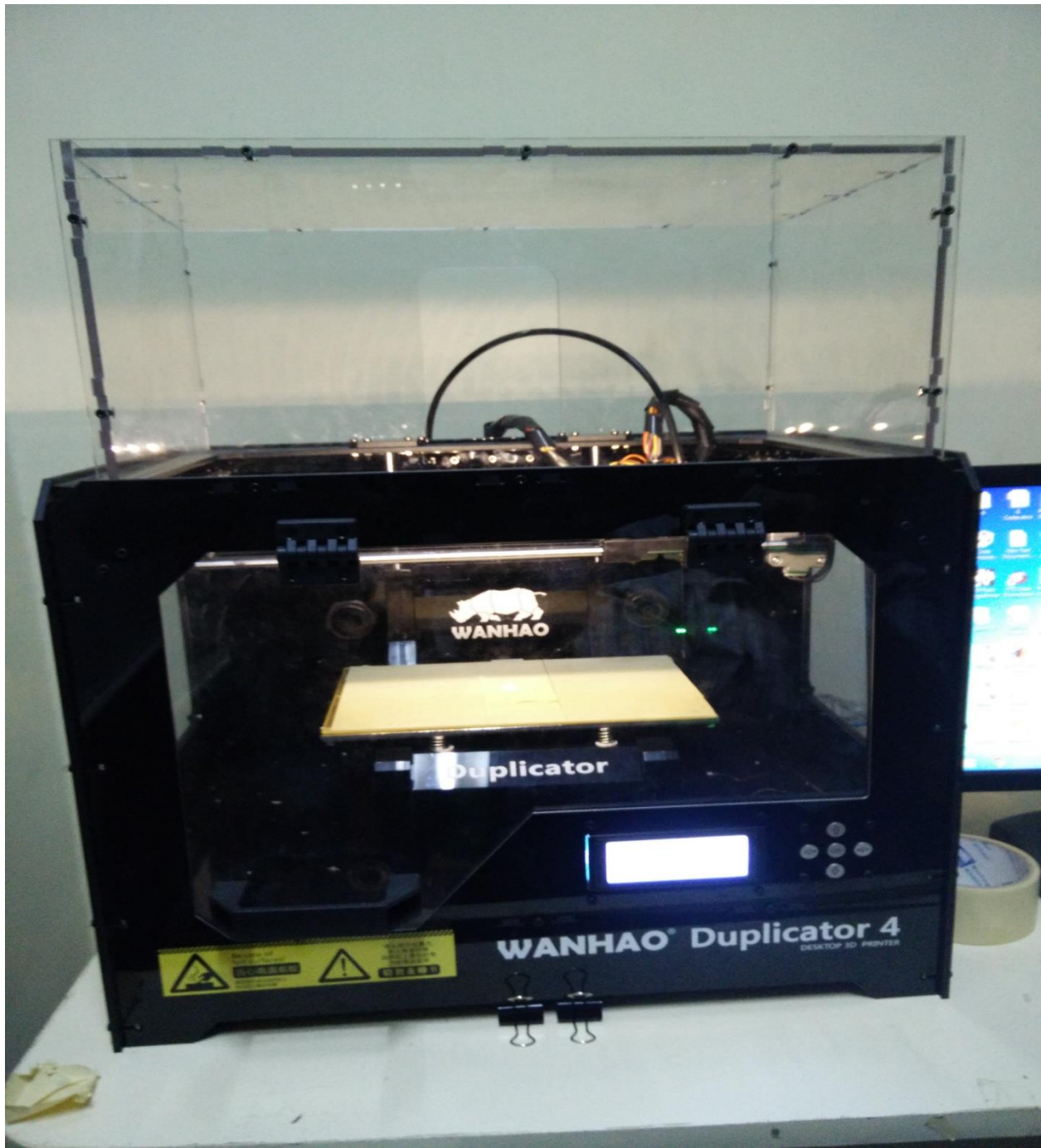


Figure 5.8: 3D printer

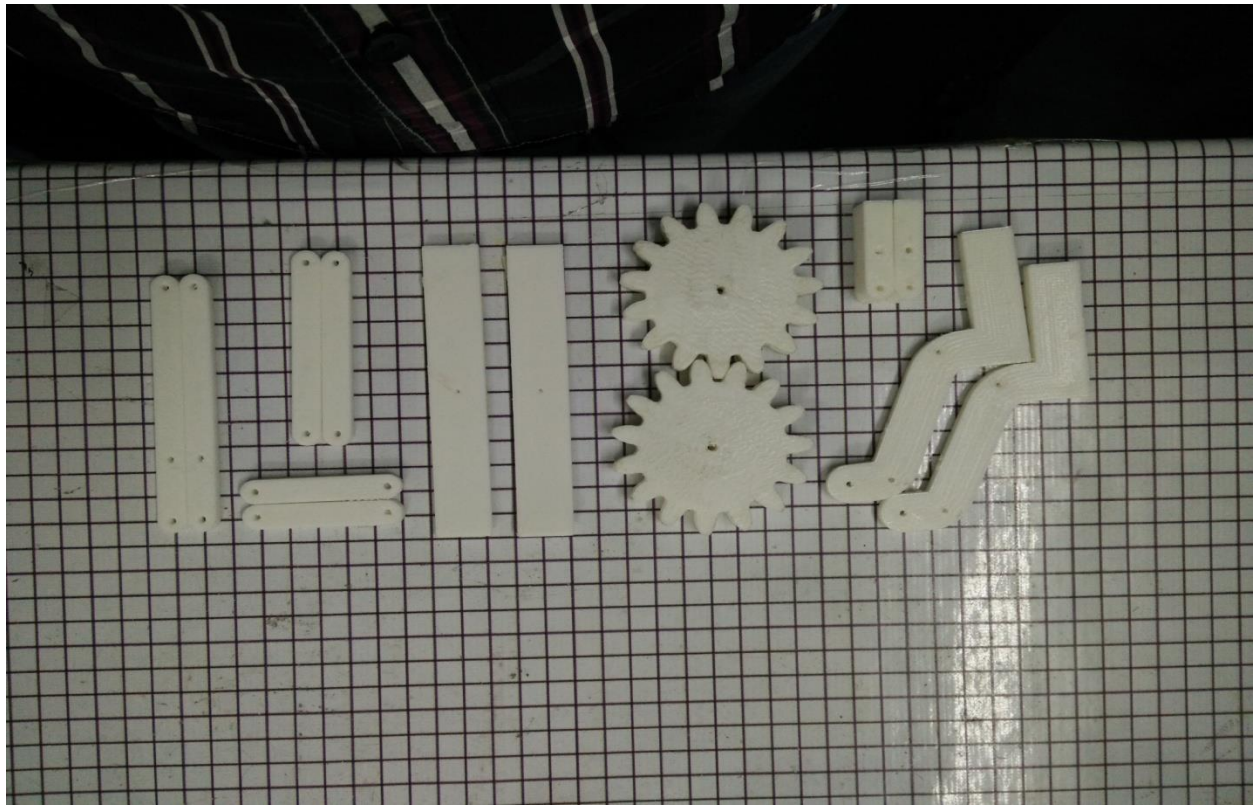


Figure 5.8: 3D printed parts of the Palm

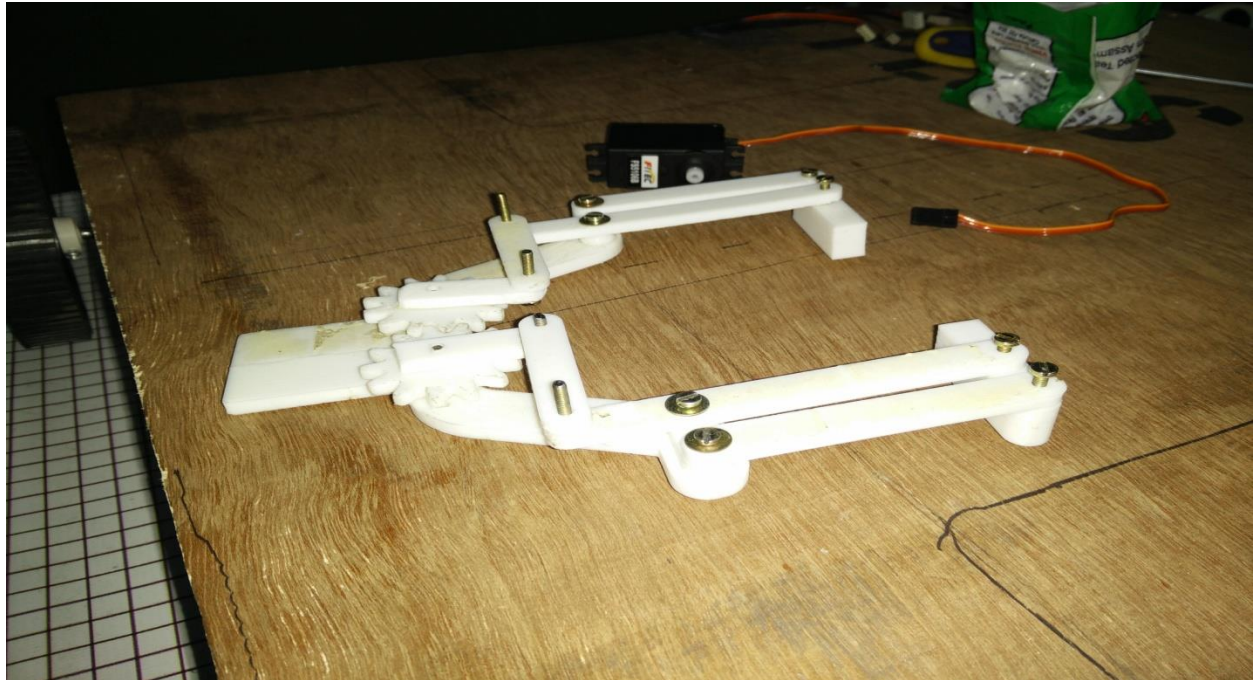


Figure 5.8: Parallel gripping palm (Without motor)

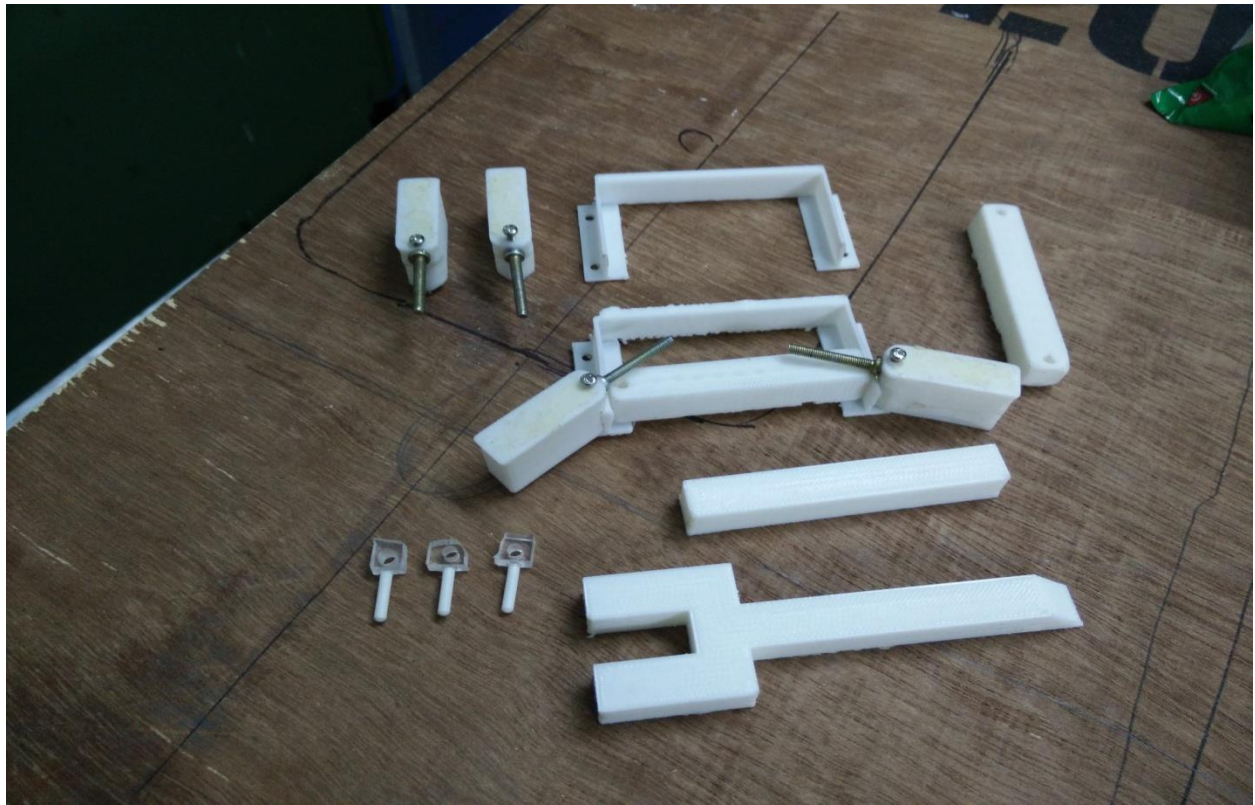


Figure 5.8: The picture shows adaptive finger assembly and the 3rd finger at the bottom

Thus after assembling the adaptive finger with the palm the light weight gripper is constructed.

6 SLAM BASED NAVIGATION

6.1 INTRODUCTION

This section describes and discusses a research work on Simultaneous Localization and Mapping with a Mobile Robot using a RGB-D Sensor. The main goal of this project is to study the use of the Kinect in mobile robotics and use it to assemble an integrated system capable of building a map of the unknown environment using visual and feedback from other sensors like optical encoders.

This work addresses the following subjects: mapping, navigation and exploration with the help of RGB-D camera (i.e.Kinect). With this purpose, the Robot Operating System (ROS) framework and a Kinect mounted on top of a mobile robot were used.

Considering that the Kinect is a cheap, low precision sensor, the main objective is to assess the usability of the Kinect to explore, navigate and map indoor, cluttered environments without the use of any further sensors, and investigate how the environmental factors, such as light and low featured scenarios, affect the results. The final and foremost objective is the integration of the aforementioned modules and the development of a mobile robotic system that autonomously navigates and maps indoor, cluttered environments.

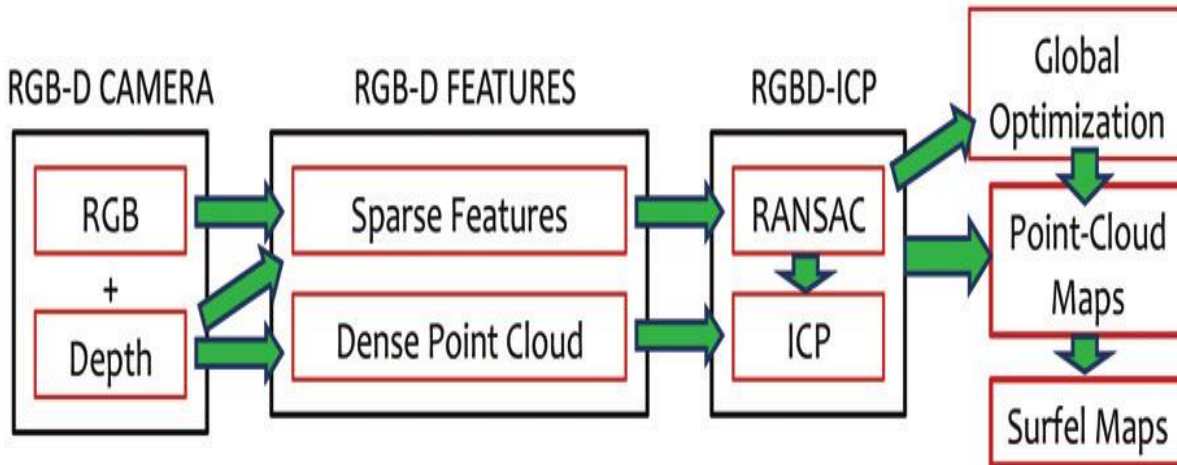
6.1.1 Related Work

Mapping

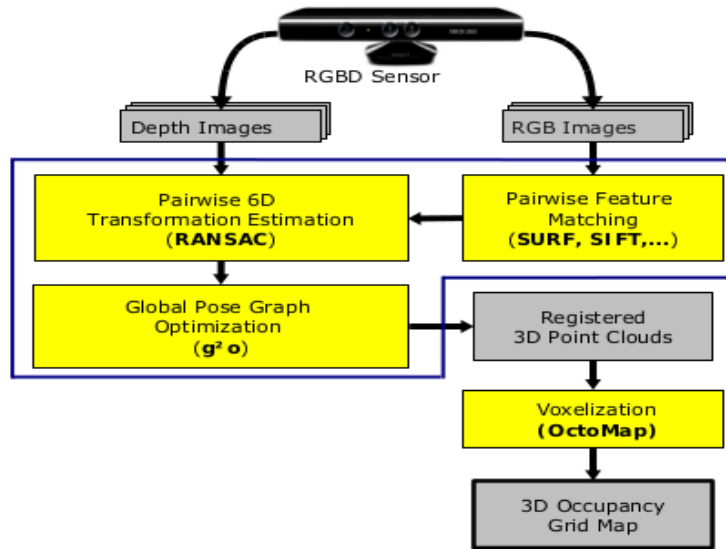
Several relevant applications in robotics require the ability to create a model of the environment and to estimate the robot's pose regarding this model. For a mobile robot, for example, it is essential to know its location in order to navigate safely to a specific target. With the arrival of cheap RGB-D sensors, an approach for Simultaneous Localization and Mapping (SLAM) can be made, combining both depth information and visual features from the RGB camera to create dense 2D or 3D environment representations. However, 3D SLAM is a task with high

computational burden, and consequently, in certain applications where the mobile robot's motion is constrained to a plane, e.g. SaR mission in a facility where a leakage of toxic substances occurred, the 3D information is projected to 2D to perform these tasks.

RGB-D Mapping



(a) RGB-D SLAM by Henry et al



(b) RGB-D SLAM by Endres et al

Figure 6.1: Overview of two different RGB-D SLAM approaches.

RGB-D mapping consists of generating dense 2D/3D models of indoor environments using both the RGB images and their corresponding per-pixel depth. Several approaches have been presented in order to obtain those models.

Figure 1a illustrates the approach presented by Henry et al. Later on, Endres et al presented a similar approach, as shown in Figure 1b, differing on the fact that they discarded the Iterative Closest Point (ICP) that Henry et al. found often unnecessary, using the g^2o framework instead, presented by Kuemmerle et al. to optimize the 3D graph pose. Also, on the post-processing step, where Endres et al. used a volumetric voxel representation that can be directly used for robot localization, planning and navigation, Henry et al. used Surfel Maps. The latter is a concise representation of the map that incorporates all the information from the RGB-D frames and it is based on surfels. A surfel consists of a location, a surface orientation, a patch size and a color.

2D Mapping

Although RGB-D sensors allow the creation of 3D models of the environment, it is a task with high computational burden, and even the fastest, state of the art algorithms represent a considerable computational cost. Therefore, in robotic applications that besides mapping, also need to perform other tasks and its movement is restricted to a 2D plane such as indoor scenarios, a projection of the 3D information to 2D might be considered, thus allowing the use of 2D SLAM algorithms. Such algorithms require a much lower slice of the computational systems' capabilities. The most popular 2D SLAM algorithms rely on probabilities to cope with noise and estimation errors. There are several implementations based on Kalman Filters and Particle 10 Filters. An alternative approach is graph-based SLAM, using pose graph optimization. In this case, algorithms use the data to build a graph composed of estimated poses, local maps and their relations, in order to compute a consistent global map. ROS, the robotic framework used on this project, already comprises a set of 2D SLAM algorithms, such as GMapping, HectorSLAM, KartSLAM, etc. HectorSLAM heavily relies on fast scan matching and does not use odometric information from the robot which makes it a viable option for aerial robotics. KartSLAM is a graph-based algorithm that employs a highly optimized

decomposition for sparse linear systems. GMapping is the most used SLAM algorithm in robotics and it is a Rao-Blackwellized Particle Filter SLAM approach. It takes the movement of the robot and previous observations into account, achieving interesting performance with a low number of particles, e.g. 30 particles.

6.2 THE MICROSOFT KINECT

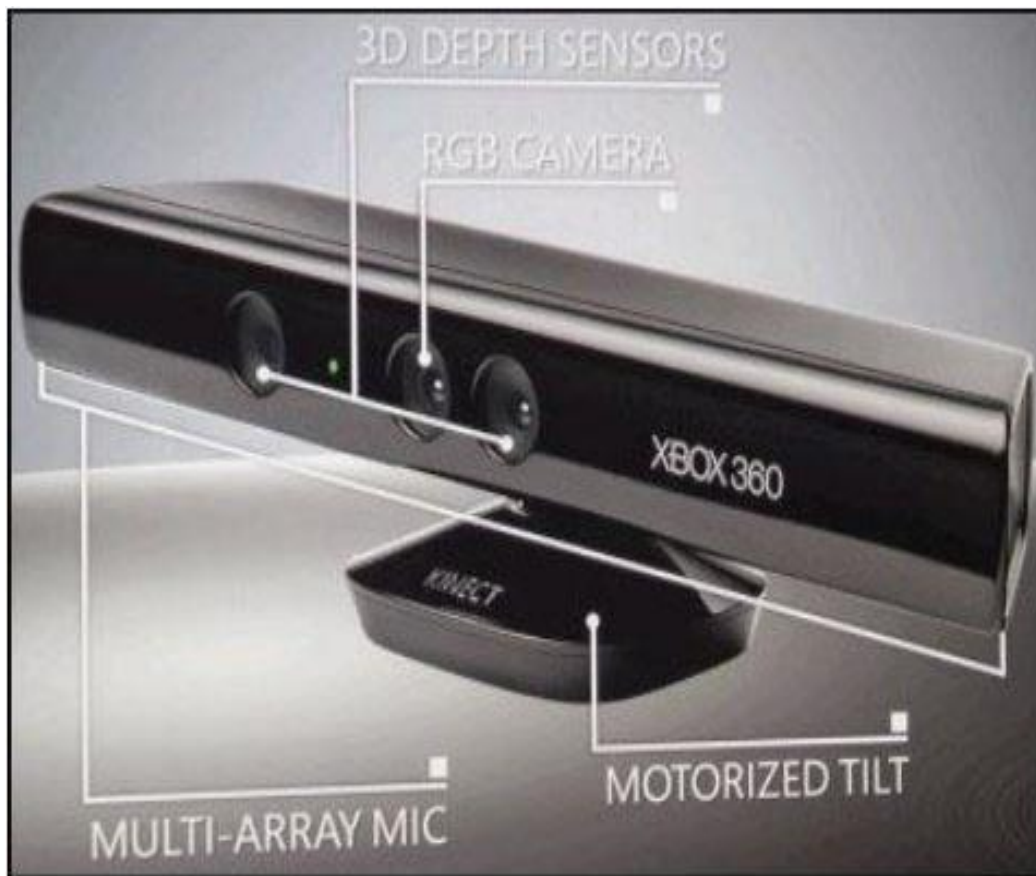


Figure 6.2: The Kinect and its main components

The Microsoft Kinect is a revolutionary sensor designed by PrimeSense and launched in 2010, being widely used in the gaming industry. However, due to its interesting features, it is also suitable for robotic use, specifically indoor navigation, mapping, people detection and tracking. It has become popular because of its low

price and its capability to provide RGB images and depth information simultaneously and even combine them to create a coloured point cloud. The basic parts of the Kinect are shown in Figure 2. These are: the MA, the motorized tilt system, the RGB camera, and the 3D depth sensors composed by an IR projector and an IR camera.

6.2.1 Depth Measurement

The depth measurement system comprises an IR projector and an IR camera. Depth measures are accomplished through a structured light technique. Cruz et al. showed that the projector emits a single beam that is split into multiple beams in order to create a pattern of speckles projected in front of the Kinect. The emitted pattern is then captured by the IR camera and is correlated against a previously defined reference pattern. Figure 3 shows an example of the pattern captured by the IR camera.

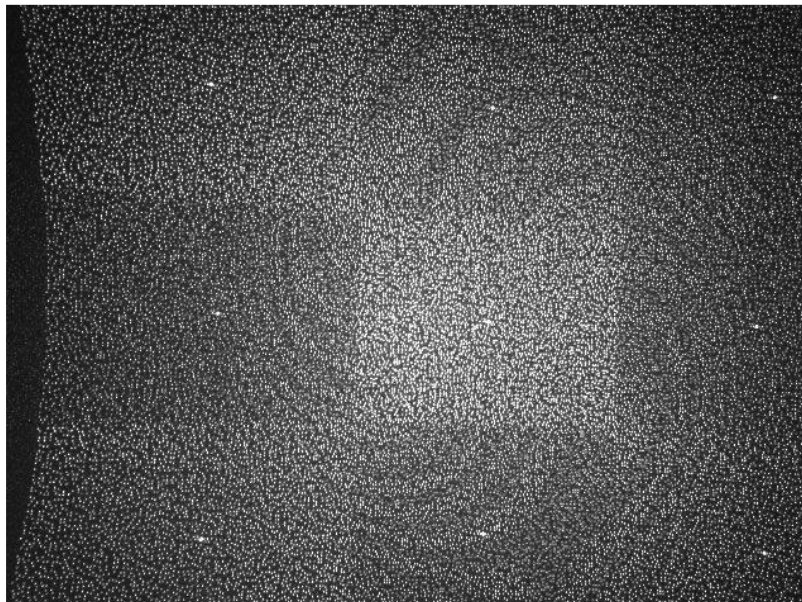


Figure 6.3: Emitted pattern of speckles by the Kinect

When a speckle is projected on an obstacle whose distance to the sensor is not the same as the reference plane with known distance, its position on the captured IR image will be shifted accordingly. By calculating the shift of all speckles, a disparity image is obtained. Then, for each pixel, given the known depth of the reference

plane and the disparity, the distance to the sensor can be computed using a triangulation model, as Khoshelham and Elberink described.

6.2.2 Triangulation model

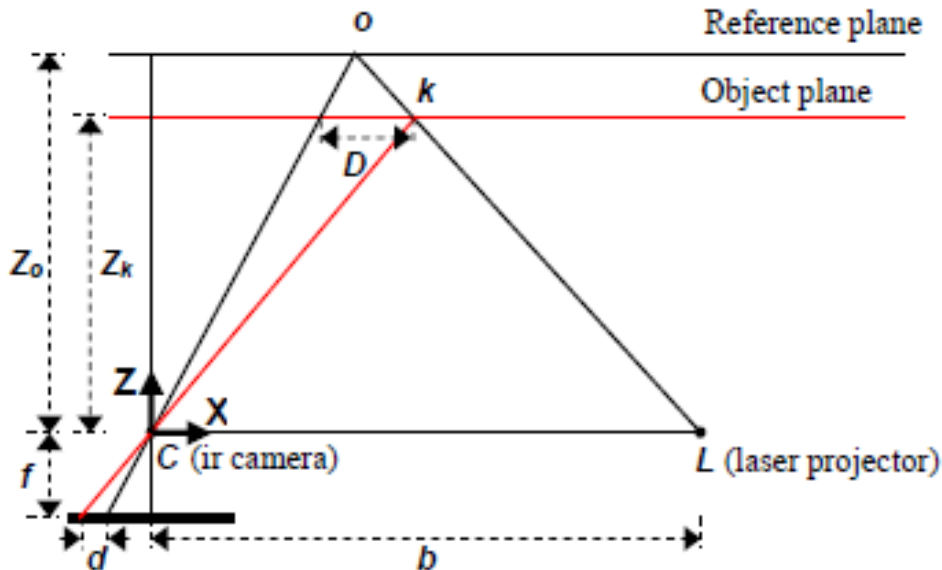


Figure 6.4: Schematic representation of depth-disparity relation

In order to compute the depth of each pixel with information of disparity and the distance between the reference plane and the sensor, a triangulation method is used.

In Figure 4, k is the point in the object plane, b is the base length, f is the focal length of the IR camera, D is the displacement of the point k , Z_k is the depth of the point and Z_o is the distance to point k 's projection on the reference plane. Z_o , f , and b are constant parameters obtained by calibration.

Figure 4 illustrates the relation between the distance of an obstacle point k to the sensor and the reference plane's projection of the same point k and their corresponding disparity d . In this schematic, we consider a depth coordinate system with its origin at the perspective center of the IR camera. The Z axis is orthogonal to the image plane and points towards the obstacle and the X axis is perpendicular to the Z axis in the direction of the baseline b between the IR camera center and the IR projector.

Considering the similarity of triangles, we have:

$$\frac{D}{b} = \frac{Z_0 - Z_k}{Z_0} \quad \dots \dots (1)$$

$$\frac{d}{f} = \frac{D}{Z_k} \quad \dots \dots (2)$$

Thus, we can obtain the depth from equations 1 and 2:

$$Z_k = \frac{Z_0}{1 + \frac{Z_0}{fb} d} \quad \dots \dots (3)$$

As a result, equation 3 provides the mathematical background to compute depth from the constant parameters Z_0 , f , and b .

With the output of these calculations along with further processing for representation, and combining with the information from the RGB camera, the Kinect provides coloured point clouds.

6.2.3 Kinect Data Accuracy

The Kinect, as well as other low-cost range sensors, is an attractive alternative to expensive LRFs and Light Detection And Ranging (LIDAR) systems. However, its accuracy has to be analyzed to assess whether it is suited for mobile robotics' use. The Kinect captures depth images at a frame rate of about 30 frames per second (fps), simultaneously with color images. Combining both information results in a coloured point cloud that contains about $300,000^2$ points for each frame.

6.2.4 Precision and Resolution

The resolution of the IR camera determines the point spacing of the depth data. The Kinect's IR camera produces a constant 640×480 pixels per frame, which led Khoshelham and Elberink to conclude that the depth resolution is inversely proportional to the distance to the sensor, i.e. the depth information is less precise for objects farther away from the sensor, and for mapping applications the range should be 1 to 3 meters. Viager concluded that the Kinect is, in general, fairly accurate for a range of 0.6 to 4.6 meters.

Specification	Value
RGB and Depth images resolution	640×480
Frame rate	30 fps
Ideal operation range	$0.6m - 4.6m$
Ideal operation range for people detection	$\approx 1m - 3m$

Table 6.1: Kinect specifications

	RGB	IR
Horizontal	62	58
Vertical	48	44
Diagonal	72	69

Table 6.2: Approximate values of the Kinect Field of View (FoV) in degrees

6.3 APPLICATIONS IN MOBILE ROBOTICS

The information provided by the Kinect is of great use in the mobile robotics field. Tolgyessy and Hubinsky further analysed this sensor to determine which applications it is best suited for, as reported in their work in. Below, some examples of applications are provided.

6.3.1 Obstacle Avoidance and Collision Detection

In order to safely navigate through any environment, a mobile robot must always protect itself from obstacles and other collisions, e.g. walls or people. Since the Kinect provides a depth map with good resolution, this information alone can be used to that end. However, the depth measurement system reveals some issues with certain obstacles, such as reflective or transparent materials and in non-ideal environments, such as those with strong lightning. Therefore, combining depth information with RGB data is beneficial. To assure the absence of collisions, it is necessary to program the robot to stop its motion and eventually re-plan its trajectory whenever an obstacle is below a safety distance. This can be achieved through the depth map by verifying the existence of pixels with depth information below the defined threshold.

6.3.2 Localization and Navigation

An autonomous robot should be able to localize itself and navigate to a precise destination. For this purpose, the information from the Kinect's depth map is useful in building a 3D or 2D map and localizing the robot, as well as avoiding obstacles and collisions as Henry et al. concluded. Furthermore, the images from the RGB camera can be combined with the depth maps for visual odometry applications, to enable more precise localization.

6.4 KINECT ON ROS

6.4.1 Robot Operating System (ROS)

Writing software for robots is a difficult task, especially with the highly varied hardware used in Robotics. Furthermore, the software must cover all levels, from driver-level, to perception and abstract reasoning. Over the years, a wide variety of frameworks have been created to ease the software prototyping.

In this context, ROS is a framework devoted to large-scale integrative robotics research and, thus, it is becoming more important as robotic systems grow in complexity. ROS is most likely not an optimal solution for particular robotic systems because of the constraints of developing a large-scale solution. However, it is suitable for virtually every system.

Quigley et al. made an overview of ROS. According to the authors, the philosophy of ROS is based on several aspects referred below.

- Peer-to-Peer: system consist of processes, called nodes that can run on different hosts;
- Multi-lingual: support various languages such as C, C++, Python, Octave, Lisp;
- Tools-based: based on a microkernel design complemented with tools;
- Thin: drivers and algorithms built in standalone libraries, i.e. easy to reuse;
- Free and Open-Source: all its source code is publicly available and developments are promoted.

6.4.2 ROS and the Kinect

As researchers started to use the Kinect in robotic systems, significant work was made using ROS. Most of which is currently available and ready to use. There are two main driver implementations for the Kinect on ROS: the freenect_stack, and the most commonly used one Openni_kinect. These drivers allow a fast collection of the information provided by the Kinect.

6.5 PROPOSED SYSTEM

6.5.1 Vision based SLAM

Many vision sensor applications have been developed in recent years due to low cost, low power consumption and development of high speed processor. In our work, conventional SLAM algorithm using the vision sensor (vSLAM) is adapted for the system integration.

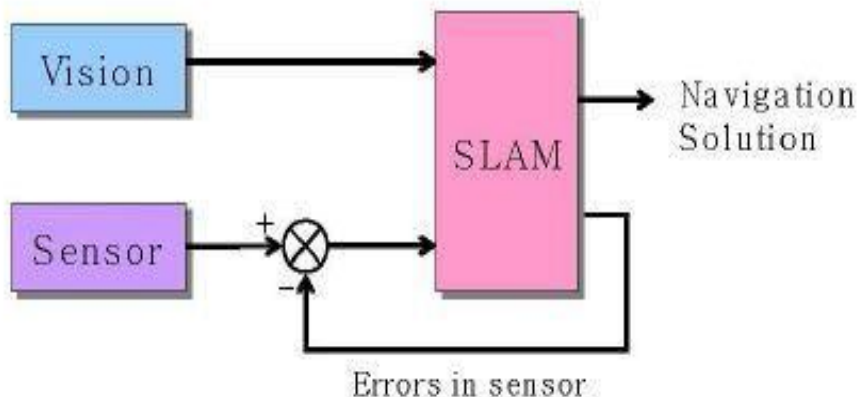


Figure 6.5: Basic concept of vSLAM

Using vision sensor, feature points are selected and tracked on continuous frames. Vision sensor also provides bearing elevation or range information of feature point, which is deduced from feature points tracking data. Other sensor output goes to SLAM block with vision sensor data. Navigation information (position, velocity, attitude, etc.) and errors in sensors are estimated by integrating information from

vision and other sensor. Assuming feature points are fixed and not movable in the local coordinate frame, navigation errors dominantly comes from sensor outputs. Thus by compensating estimated errors from sensor output, navigation data can be calculated precisely.

6.5.2 Odometry System

As shown in Fig 6, the mobile robot has two drive wheels and two castors. The two drive wheels are connected to DC motors with 15-bit quadrature encoders. These encoders are capable of monitoring the revolutions and steering angles of the drive wheels. The main advantage offered by these encoders is their high resolution. The odometry is implemented using the results from these encoders. The two output channels of the quadrature encoder indicate both position and direction of rotation.

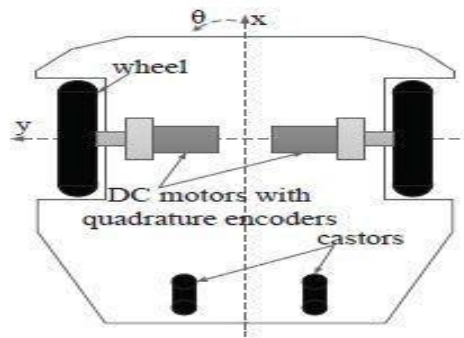
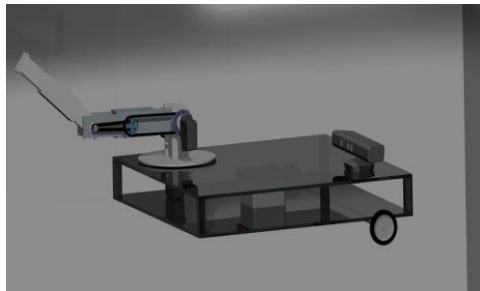


Figure 6.6: Odometry system

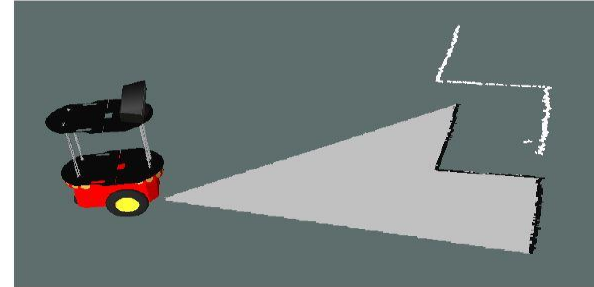
6.5.3 Mapping

Although the Microsoft Kinect allows to perform RGB-D mapping, our goal is to run a SLAM algorithm along with other tasks, such as autonomous exploration.

Considering performance constraints, the option was to project the depth measurements provided by the sensor in the floor plane and simulate a 2D laser scan. This is represented by the *Depth to LaserScan* block and by the *depthimage_to_laserscan* ROS node. It processes the columns of the image matrix and creates a vector with the minimum depth value per column, thus originating a vector of 640 distance readings, i.e. a 2D scan.



(a) Mobile robot platform with Kinect on the top



(b) Laser scan output from rviz: robot model, map and laser scan in white

Figure 6.7: Photo of the hardware and the output in rviz of the mapping module.

The 2D range measurements are then used as an input to the *GMapping* SLAM algorithm, available in ROS, along with odometry information provided by the robot's driver.



Figure 6.8: RGB image on the left and depth image on the right

This SLAM algorithm was selected for several reasons. Firstly, considering the performance constraints, it does not present a high computational burden. Secondly, the Microsoft Kinect has a low Field of View (FoV), which can cause problems in scan matching, therefore the mobile robot's odometry can greatly improve results. Finally, it was shown to be robust in testing and experiments, when compared to other SLAM approaches. Despite the result being a 2D map, using the Kinect yields an advantage the map contains 3D information, since the projection from the depth image to a simulated laser scan uses the depth information available from the sensor.

7 RESULTS

A model for the material handling system was designed and fabricated. The adaptive gripper is capable of handling various object shapes up to 12 centimeters. It also eliminates the moment handling problems as in case of two finger grippers. The robotic arm developed has a better accuracy in positioning and lower inertial drift as the centre of gravity is low, because of the belt drive arrangement.

A 2D map of the room was developed by implementing the Simultaneous Localization and Mapping algorithm on the Robot Operating System (ROS). This algorithm involves less computational efforts and thus served to be the best option for adaptive autonomous navigation.

8 FUTURE SCOPE

The positional errors of the end effector may be due to the inherent errors of the Kinect and the mechanical errors introduced due to the motors, belt drive, etc. To reduce these errors an artificial neural network based error compensation method can be implemented in which the neural network predicts the errors at various configurations and the controller takes these predictions into account for the positioning of the end effector.

A scaled up robot can be used for material handling in industries where a large number of projects are to be handled simultaneously, as it reduces manpower, is capable of adapting to different environments and works with high efficiency.

9 BIBLIOGRAPHY

- [1] R. K. Mittal, I. J. Nagrath, "Robotics and Control", McGraw Hill Edu. Pvt. Ltd, 2013
- [2] K. Goyal, D. Sethi, "An analytical method to find workspace of a robotic manipulator", Journal of Mechanical Engineering, Vol. ME 41, No. 1, June 2010, Transaction of the Mech. Eng. Div., The Institution of Engineers, Bangladesh, pp. 25-30.
- [3] K. Khoshelham, "Accuracy analysis of kinect depth data", International Archives of the Photogrammetry, Remote Sensing and Spatial Information Sciences, Volume XXXVIII-5/W12, 2011, ISPRS Calgary 2011 Workshop, 29-31 August 2011, Calgary, Canada, pp. 133-138.
- [4] O. Kisi, E. Uncuoglu, "Comparison of three back-propagation training algorithms for two case studies", Indian Journal of Engineering & Materials Sciences, Vol. 12, October 2005, pp. 434442.
- [5] G. J. Monkman, S. Hesse, R. Steinmann, H. Schunck, "Robot Grippers", 2007:Wiley
- [6] C. Xiong, "Fundamentals of Robotic Grasping and Fixturing", Huazhong University
- [7] R. Ricard, C. M. Gosellin, "On the Determination of the Workspace of Complex Planar Robotic Manipulators", ASME Journal of Mechanical Design, Vol.120, 1998, pp.269-278.
- [8] K. Kumar, Waldron, "The Workspace of a Mechanical Manipulator", ASME Journal of Mechanical Design, Vol.103, 1981, pp.665-672.
- [9] B. Freedman, A. Shpunt, M. Machline, Y. Arieli, "Depth mapping using projected patterns", Prime Sense Ltd, United States, 2010.
- [10] P. Henry, M. Krainin, E. Herbst, X. Ren, D. Fox, "RGB-D Mapping: Using Depth Cameras for Dense 3D Modeling of Indoor Environments", Proc. of International Symposium on Experimental Robotics (ISER), Delhi, India, 2010.
- [11] T. Tamamoto, K. Sayama, K. Koganezawa, "Multi-Joint Gripper with Differential Gear System", 2014 IEEE/RSJ International Conference on Intelligent Robots and Systems (IROS 2014), September 14-18, 2014, Chicago, IL, USA, pp. 15-20.

- [12] M. Wassink, R. Carloni, S. Stramigioli, “Port-Hamiltonian Analysis of a Novel Robotic Finger Concept for Minimal Actuation Variable Impedance Grasping”, IEEE Intern. Conf. on Robotics and Automation, pp. 771-776, 2010.
- [13] D. Fox, W. Burgard, F. Dellaert, S. Thrun, “Monte carlo localization: Efficient position estimation for mobile robots”, In Proceedings of the National Conference on Artificial Intelligence, JOHN WILEY & SONS LTD, 1999, pp. 343–349.
- [14] H. Durrant-Whyte, T. Bailey, “Simultaneous localization and mapping (slam): Part i the essential algorithms,” IEEE Robotics and Automation Magazine, vol. 2, 2006, pp. 1–9.
- [15] T. Bailey, H. Durrant-whyte, “Simultaneous localization and mapping (slam): Part ii state of the art,” Computational Complexity, vol. 13, no. 3, 2006, pp. 1–10.